THE CORROSION OF ZINC-STAINLESS STEEL COUPLES IN FLOWING SEA WATER

BY

HENRY SHAW

A THESIS
PRESENTED IN PARTIAL FULFILLMENT OF
THE REQUIREMENTS FOR THE DEGREE
OF
MASTER OF SCIENCE IN CHEMICAL ENGINEERING
AT
NEWARK COLLEGE OF ENGINEERING

Newark, New Jersey
1962

ABSTRACT

The effect of sea water flow on passivated stainless steel 304 coupled to high purity zinc was studied for more than 1000 hours at 23°C. The corrosion of both members of the couple increased over that of the metals alone. Zinc suffered severe pitting while the Stainless Steel was not visibly corroded. When the metals were exposed alone, zinc corroded uniformly while the stainless steel was not affected at all. The use of zinc coupled to Stainless Steel is not recommended in systems exposed to sea water.

APPROVAL OF THESIS

FOR

DEPARTMENT OF CHEMICAL ENGINEERING
NEWARK COLLEGE OF ENGINEERING

BY

FACULTY COMMITTEE

APPROVED: ______________________________

____

____

NEWARK, NEW JERSEY
JUNE, 1962

ACKNOWLEDGMENT

The author is indebted to the Socony Mobil Oil Co. for providing space and equipment to accomplish this research. Numerous co-workers at the Stony Brook Research Laboratory and at the Industrial Reactor Laboratories offered many valuable suggestions. Mr. Vincent Lafferty and Mr. Phillip Garrison helped with equipment construction and specimen fabrication. Mr. Daniel Arbach helped with photography. Miss Mary Craven did the typing. Mr. W. E. Smith's suggestions in equipment design were invaluable. Special thanks are extended to Dr. Charles L. Mantell for suggesting and guiding the research for this thesis.

The New Jersey Zinc Company, The National Lead Company and Whitehead Metals, Inc. supplied the specimens for this research. The Lake Products Company supplied the salt mixture for making the synthetic sea water.

TABLE OF CONTENTS

LIST OF FIGURES

LIST OF PHOTOGRAPHS

LIST OF TABLES

INTRODUCTION

Corrosion involves the transformations of materials of construction from refined or purified states back to natural states. The concept of corrosion as a reversion from the metastable condition of the metal to the stable condition of the mineral with the accompanying reduction in free energy is now generally accepted.

Evans(3) established that underwater corrosion is essentially electrochemical in nature. When two dissimilar metals are contacted in an electrolyte, electrons pass through the metallic parts from anode to cathode while ions balance the charge by passing through the electrolyte in the reverse direction.

In neutral or basic salt solutions, such as sea water, the accumulation of electrons in the cathode is counteracted by oxygen. The oxygen in turn is reduced as:

$$4\ e^- + O_2 + 2H_2O \longrightarrow 4\ (OH)^-$$

This constitutes the oxygen absorption type of corrosion. The formation of hydroxyl ions at the cathode must correspond to the development of free alkali. In static systems this tends to accumulate near the cathode and affect subsequent attack. The corresponding anodic product is a soluble salt of the metal. In the case of stainless steel cathodes and zinc anodes the chemistry can be described as:

$$\text{(anode) } 2Zn - 4e^- \longrightarrow 2Zn^{++}$$

$$\text{(cathode) } 4e^- + O_2 + 2H_2O \xrightarrow{ss304} 4(OH)^-$$

The corrosion products for zinc in dilute solutions of sodium chloride were shown by W. Feinknecht(4) to follow accepted thermodynamic principles. These general principles are discussed by M. J. N. Pourbaix(11) in "Thermodynamiques des Solutions Aqueuses Dilues". Pourbaix made use of potential - pH diagrams to depict regions within which immunity, corrosion or passivation may be expected to prevail.

The distribution of corrosion products is the predominant factor in determining the course of attack for any metal environment. This distribution may range from a superficial attack through varying degrees of localization to the "pitting" type of attack. Large cathode areas and small anodes areas also result in a large rate of penetration for a given metal loss.

Sea water induced corrosion is characteristic of both air saturated and electrolytic corrosion. Inherently, air saturated sea water is no more corrosive than air saturated fresh water. But the current of galvanic and concentration cells can flow through greater distances in sea water and, therefore, the cathodic area of a cell may become relatively large, and the corrosion more intense.

Stainless steel finds little use in marine applications mostly because of its high relative cost. There are some applications in which stainless may have some inherent advantages such as in fuel tanks of large ships where sea water is run in as the fuel is used up. Other areas in which stainless steel is used include propellers for ships and off-shore oil drilling apparatus. The current plans for saline-conversion demonstration plants include much stainless steel equipment. It would be desirable to determine if a sacrificial anode such as zinc, would add to the life of this type of equipment.

Zinc plates have been used for many decades as protection for steel in marine applications. Bannister(1) points out that the protection so afforded is not electrolytic but is due rather to using up the oxygen in the water by the normal uncoupled corrosion of the zinc. The oxygen thus becomes unavailable for steel corrosion.

Since the high corrosion resistance of stainless steel depends on maintaining a good oxide film, it is desirable to maintain oxygen available to the film in order to repair any discontinuities. Also, various workers in corrosion claim that stainless steel pits when exposed to sea water. The effect of zinc on the corrosion of stainless steel in flowing, aerated sea water is, therefore, of more than pure academic interest.

EXPERIMENTAL PROCEDURE

The design of this experiment can be divided into four parts. Part one involves the selection of experimental conditions, Part two describes the design and operation of the flow loop. Part three describes the design and operation of the static experiment. Part four describes the specimen preparation and assembly.

Selection of Experimental Conditions

There are many factors which effect the corrosion of metals. A conscientious effort was made to minimize the number of variables in this study and thus allow a greater degree of reproducibility. Synthetic sea water was used instead of natural sea water for this reason.

The sea water was made with "Sea-Rite", a commercial salt mixture which contains all the elements found in natural sea salt in quantities greater than 0.004%. The specified composition of the salt is tabulated below:

TABLE 1

Sea-Rite Salt Composition

Sodium	30,577%
Magnesium	3.725%
Calcium	1.178%
Potassium	1.009%

Strontium	0.038%
Boron	0.0135%
Chloride	55.035%
Sulphate	7.692%
Bromide	0.1868%
Bicarbonate	0.405%
Fluoride	0.0039%

The Lake Products Company, manufacturers of Sea Rite, suggests the use of tap water to mix the sea solution provided it contains less than 500 parts per million total solids. Otherwise, they recommend distilled water. In order to obtain an average composition of sea water, Sea Rite was mixed to a concentration of 4-1/2 ounces per gallon of tap water. The tap water contained an unusually high iron concentration although the total solids were well below 400 parts per mission. When the solution was mixed, the iron precipitated as a hydroxide because of the alkalinity of the salt solution. This brown precipitate was maintained in suspension due to the high rate of circulation in the corrosion loop. The effect of having this precipitate on the corrosion tests was not determined but was assumed negligible. Speller(13) indicated that one-thousandth percent of iron in water gives an oxidizing capacity several times that of air. However, iron in chloride systems is very protective to stainless steel. The effect of iron on zinc is not known. At any rate, it is not expected to behave in a way much different than suspended matter in natural sea water.

A sample of the sea water was analyzed by the Drew Chemical Corporation and reported the following:

TABLE 2

Water Analysis at Termination of Experiment

pH	8.6
Total Hardness (as $CaCO_3$) in p.p.m.	1890
Calcium (as $CaCO_3$) in p.p.m.	280
Magnesium (as $CaCO_3$) in p.p.m.	1610
Chloride (as Cl) in p.p.m.	11,900
Sulfate (as SO_4) in p.p.m.	1100
Silica (as SiO_2) in p.p.m.	4.9
Conductivity in Micromhos (m.m.h.)	<10,000
Suspended Solids in p.p.m.	41
Iron (as Fe) in p.p.m.	6.0
Visual Appearance	Amber
Specific Gravity	1.015

Using the data of Table 3, one can determine the characteristics of sea water. Uhlig(14) lists the properties of sea water as a function of salinity or chlorinity.

Salinity = 0.03 + 1.805 x chlorinity

Salinity = total amount of solid material in grams contained in one kilogram of sea water when all carbonate has been converted to oxide, the bromine and iodine replaced by chlorine, and all organic matter is completely oxidized.

Chlorinity = total amount of chlorine, bromine and iodine in grams contained in one kilogram of sea water, assuming that the bromine and the iodine have been replaced by chlorine.

The data for 20°C and 25°C is reported in the following table:

TABLE 3

Synthetic Sea Water Properties

	20°C	25°C
Chlorinity	12	12
Salinity	21.7	21.7
Specific Conductance (reciprocal ohm-cm)	0.031109	0.034489
Density (g/cc)		
Salinity = 20	1.01341	1.01720
Salinity = 25	1.01210	1.01585
Oxygen Dissolved (ppm)		
Chlorinity = 10	8.21	7.48
Chlorinity = 15	7.77	7.04

The area of both specimens was kept the same in order to minimize the effect of a high cathode current density and resulting polarization when the anode is too large.

Conversely a smaller anode may not have lasted the duration of the test. Whitman and Russel(15) illustrated the effect of cathode area in the galvanic corrosion of iron-copper couples. They showed the rate of corrosion to be directly proportional to the ratio of cathode to anode area. (Copper area to iron area).

The oxygen concentration was maintained constant by allowing the sea water to drop approximately one foot in air. Oxygen will increase the depolarization of the cathode and is, therefore, desirable in solution. Bengough and May(2) indicated that air bubbles can remove protective coatings more effectively than water alone. Any entrained air was released in this experiment by allowing a settling period in the second 55 gallon drum prior to circulating through the corrosion loop, minimizing this air bubble effect. Oxygen is also desirable in systems which contain stainless steel since the relative nobility of this material is strongly dependent on its impervious oxide coating. The oxygen tends to maintain the coating in a state of repair. The concentration of oxygen in this experiment is estimated based on Henry's law from the data of Pray, et al(12) and the relative solubility of oxygen as a function of salt concentration from Speller(13) at seven parts per million. This number being in good agreement with those of Table 3 based on Uhlig(14).

In order to increase the reliability of the results the test was planned as a long time test. The initial rate of corrosion is usually much higher than after a state of equilibrium has been established and permanent coatings have started to form. The slowing down of the rate of corrosion is nearly always due to the accumulation of corrosion products on the surface of the metal. This experiment was planned for 1000 hours (42 days) and taking data points once a week for six weeks. It was assumed that a state of equilibrium would have been achieved in this length of time.

The sea water velocity effect on the corrosion of the zinc-stainless steel 304 couple was determined at the inception of turbulent flow. This flow, which corresponds to one foot per second in 1/2 inch pipe, was used in order to allow for good diffusion of corrosion product from the zone of reaction and maintain a constant oxygen supply at the zone of reaction. Care had to be exercised to ascertain that both members of the metallic couple were subjected to the same flow. Speller(13) indicated that in the absence of oxygen an area of a particular metal subjected to the higher flow rate would be anodic to the rest of the metal but in the presence of oxygen this area would be cathodic because the depolarization reaction would predominate. It was also decided to do a limited beaker corrosion

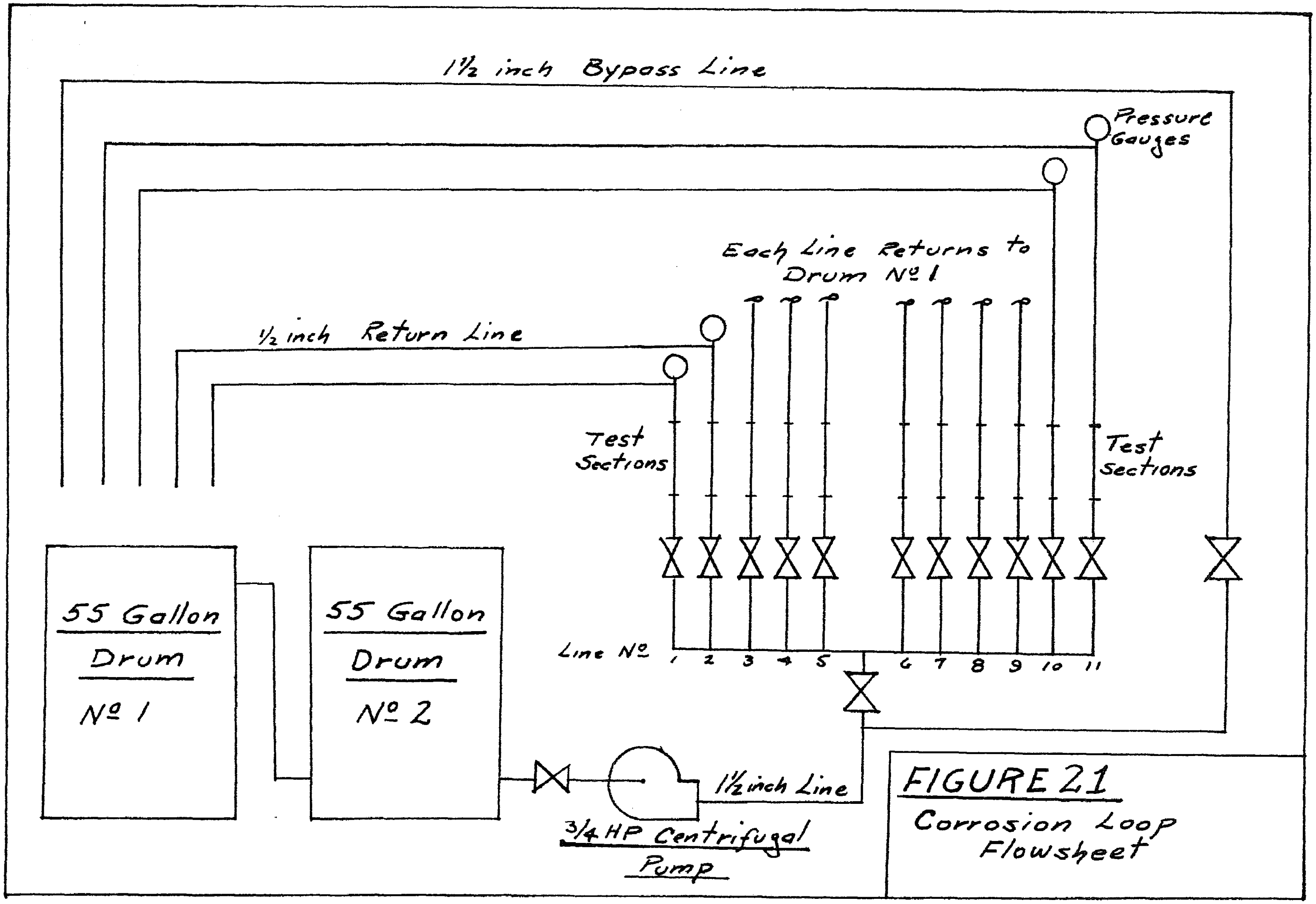

FIGURE 21
Corrosion Loop Flowsheet

test in order to compare the flow effect with static conditions.

Design of Dynamic Corrosion Experiment

The corrosion flow experiment was designed so that flow through any leg would be at least one foot per second. The volume of the system was made so large that the contribution of corrosion products to the solution would be negligible. The materials of construction had to be carefully picked so that they would resist sea water corrosion and would not influence the experiment.

The system piping was unplasticized polivinyl chloride. The valves were made of bronze. A Worthington 30 GPM stainless steel centrifugal pump was used to circulate the sea water. Two 55 gallon epoxy lines drums were used as sea water reservoirs. See Figure 21 for the loop flow sheet.

The test legs were built vertically to assure a more uniform velocity distribution through the test sections. Each test leg was made with 1/2 inch schedule 80 pipe and contained a globe valve, two unions and a pressure gauge. The test section, some seven inches long, was inserted or removed through the unions. Each leg returned individually to the sea water reservoir to allow for a direct and accurate flow measurement. The rest of the system piping was

PHOTOGRAPH 1

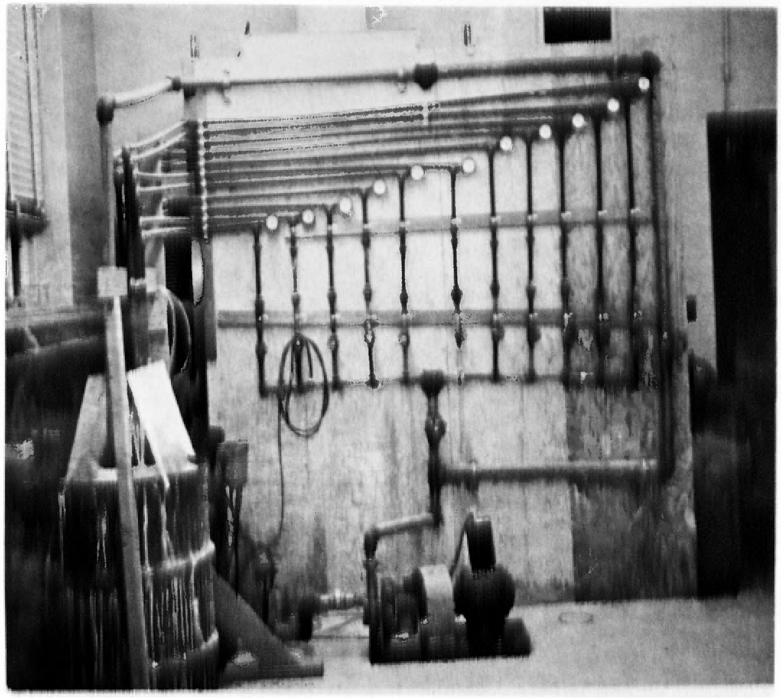

Corrosion Loop in Operation

PHOTOGRAPH 2

Return Line Aerating Section

1-1/2 inch schedule 80.

When the loop was checked out prior to starting the experimental work, it became obvious that pump vibrations would change the valve opening. In order to overcome this effect, small diameter pipe were placed at the end of each test leg to act as orifice plates. The desired flow was obtained and maintained in this manner. The valves were used only for on-off type operation.

Photographs 1 and 2 illustrate the corrosion loop in operation.

Design of Static Corrosion Experiment

The static experiments were performed in beakers. Each beaker contained only one couple or specimen under test. The sea water used in the beakers was taken from the sea water reservoir drums. The iron hydroxide precipitate settled in the beaker test thus eliminating this unknown. The type of corrosion occuring in a static experiment is inherently different from its dynamic counterpart, mostly in that a thick corrosion product laver can form and prevent oxygen access to the zone of reaction.

Specimen Preparation and Assembly

The stainless steel 304 specimens were made from a 1/16 inch sheet supplied by Whitehead Metals, Inc. from their heat number 49114. Specimen were cut 1/2 inch by 3 inches and holes drilled 1/2 inch from each end and centered. The samples were marked for identification with stamped number in four places near the holes. The specimens were then thoroughly cleaned and degreased and brightened with very fine emery cloth. The stainless steel was then passivated by exposing to 30% nitric acid for one hour. Fontana(5) has taken vigorous exception to this method of passivation although he admits it is a common practice which does no harm. Uhlig(14), on the other hand, still recommends this treatment. Since all the literature on the subject of passivation seemed to indicate that no detrimental effects will result this was done.

The specimens were washed with distilled water and acetone and dried under an infra-red lamp. The specimens were then weighed and measured and stored in a desiccator

The zinc specimens were supplied by the New Jersey Zinc Company already cut 1/2 inch by 3 inches by 1/16 inch. This Special High Grade zinc (better than 99.99% purity) is identified as N1607 in the supplier Research records. The zinc contained no more than 5 parts per million iron, 8 parts per million lead and 9 parts per million cadmium.

PHOTOGRAPH 3

Assembly Method for Specimens Connected with Stainless Steel 304 Bolts

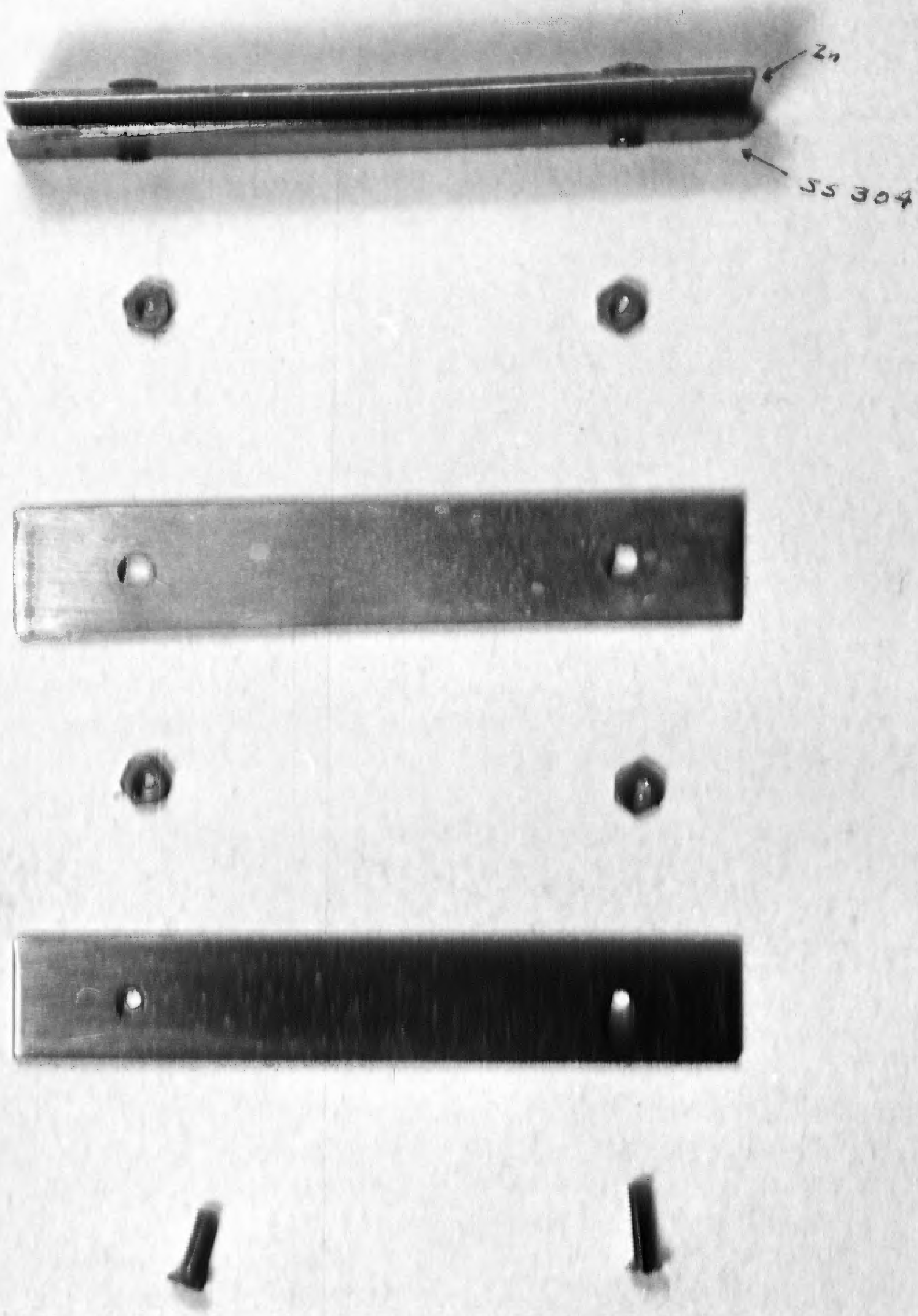

PHOTOGRAPH 4

Assembly Method for Specimens Connected with Tygon Insulated Bolts

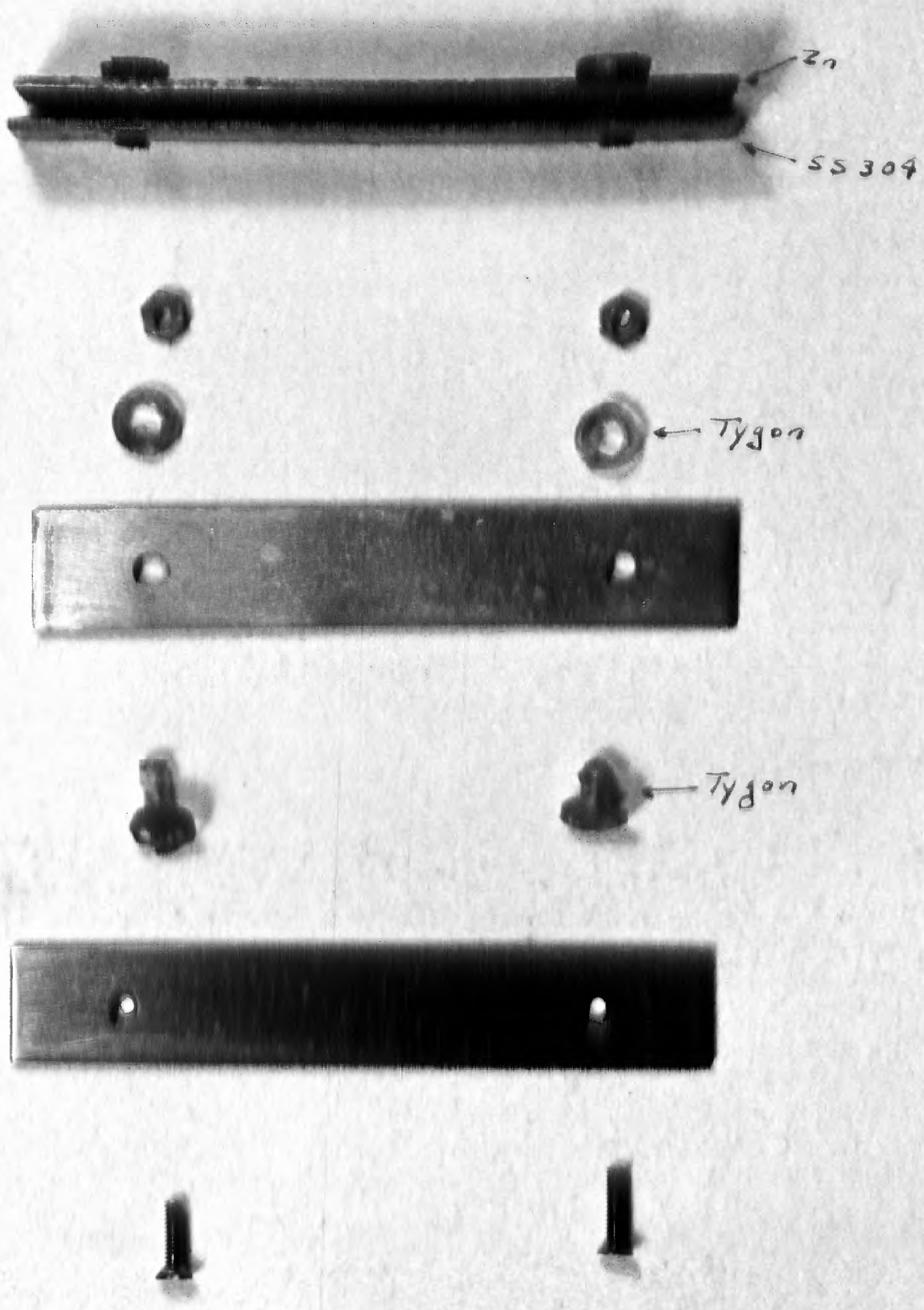

Holes were drilled in the specimen 1/2 inch from each end and centered. The specimens were then stamped in four places near the holes and cleaned with fine emery cloth. This was followed by washing with distilled water and acetone and drying under an infra-red lamp. The samples were then weighed and measured and stored in a desiccator.

The specimens were assembled either by bolting with size 2, threads 56, stainless steel 304 screws. Using a stainless steel 304 nut as a spacer, or by bolting with size 2, threads 56, stainless steel screws which were carefully covered with tygon tubing and larger diameter tygon tubing was used as a spacer. These two assembly methods are illustrated in Photographs 3 and 4.

The success of the insulation was determined by measuring the resistance between the two metals of the couple in sea water. The resistance was generally greater than 1000 ohms, using a Simpson meter, type 260, as the measuring instrument. The resistance of the directly coupled set of specimens was less than one ohm.

The post corrosion treatment of all specimens was identical. They were brushed with a steel brush, washed with water and acetone, and dried under an infra-red lamp. They were weighed and stored in a desiccator.

The voltage of the corroded specimen was measured with a Leeds and Northrup Potentiometer, using a saturated calomel electrode as a reference. This measurement was discontinued when it became obvious that a correlation would not be obtained.

The temperature in both the static and dynamic corrosion set-ups was measured at least twice weekly and it was 23 ± 1°C throughout the period of this experiment. The specific gravity of the sea water was measured every time temperature was measured with a hydrometer and it was a constant 1.02 for this experiment.

All specimens were examined with a Unitron BMEC-3 Metallurgical Microscope. The microscope did not reveal any unusual information and for brevity this information is omitted.

RESULTS

The results reported in this thesis are consistent with most corrosion research in that there is considerable scatter in the data. In spite of this, engineers have reduced similar data to quantitative functions which, with suitable safety factors, have proved invaluable in the design and operation of chemical plants.

The graphs which follow are based on the arithmetic average weight change data of two specimens although the tables list the individual specimen data. The time each specimen was exposed is reported to the nearest whole hour. The data are predicted accurate to better than five milligrams per square decimeter. This was accomplished by weighing the specimen to metter than half a milligram and measuring the specimen to better than one millimeter. The areas were not measured after corrosion because in most cases pits had developed in the zinc. The data are, therefore, based on the initial area exposed to the sea water.

In the process of analyzing the data, some analytic functions were generated which fit the weight change data well and are, therefore, reported. Caution must be exercised in using those functions since they are believed to apply only to the region where the data were obtained.

The procedure followed in obtaining these expressions was based on fitting the corrosion rate versus time plots with the best straight line. In some cases a non-linear function is strongly suggested. The equation of this line was equated to the corrosion rate as follows:

$$\frac{dw}{dt} = mt + b \qquad (1)$$

where:

w = weight change in grams per square decimeter
w' = weight change in milligrams per square decimeter
m = slope of line
t = time in hours
b = intercept of ordinate w

In most of this work the slope m was negative indicating a decrease of corrosion rate with time. The general solution of equation (1) is:

$$w = \frac{mt^2}{2} + bt + c \qquad (2)$$

where c is a constant of integration which drops out with the boundry condition that w is zero when t is zero. Equation (2) describes a parabola with the vertex in the increasing w direction, concave down. Evans$^{(3)}$ describes some work in the oxidation of metals which resulted in parabolic weight change data but he indicated that the corrosion rate expressions were hyperbolic. A hyperbolic corrosion rate indicates a high initial rate which drops off with time. This may possibly have occured in these sea water corrosion experiments but no data was taken at short exposure times. The parabolas that Evans predicts have their vertex at the origin. The theoretical implications of parabolic weight change data involves the formation of protective films on the corroding metals, thusly decreasing the rate of corrosion.

This part of the thesis is divided into three sections. Each section compares the effect of sea water velocity on the members of the galvanic couple for the three methods of couple assembly, direct connection with stainless steel 304 bolts, assembly with stainless steel 304 bolts which have been insulated with tygon and the metals themselves.

Photographic enlargements (approximately 50%) of the zinc corrosion specimens from the flow experiment are included. It is interesting how the degree of pitting can indicate the exposure time and exposure conditions of all the photographs of this section.

Velocity Effect on Stainless Steel Connection

Table 4 summarizes the weight change data for zinc-stainless steel 304 couples which were directly connected with stainless steel 304 bolts.

TABLE 4

The Sea Water Corrosion of Zinc-Stainless Steel 304 Specimens Coupled with Stainless Steel 304 Bolts at 23°C.

		Zinc			Stainless Steel		
Time hrs	Flow Rate ft/sec	Weight Loss g/dm^2	Rate mdd	Potential(1) volts	Weight Gain mg/dm^2	Rate mdd	Potential(1) volts
				Static			
283	0	0.197	17.38	1.068	2.64	0.112	0.315
283	0	0.213		1.051	0.00		0.225
598	0	0.490	18.94	1.058	14.02	0.551	0.297
598	0	0.453		1.068	13.44		0.281
839	0	0.614	16.87	1.071	20.21	0.571	0.215
839	0	0.565		1.071	19.73		0.221
1090	0	0.926	19.57	1.058	23.05	0.519	0.210
1090	0	0.852		1.092	24.09		0.220
				Dynamic			
168	1.90	2.03	297	1.010	2.60	0.826	0.210
168	1.90	2.12		1.020	9.95		0.220
339	1.80	4.54	317	1.000	8.36	0.974	0.210
339	1.80	4.41		1.050	19.16		0.210
525	1.84	4.35	194	1.079	8.99	0.900	0.300
525	1.84	4.14		1.081	30.39		0.210
665	1.86	7.20	285	1.068	25.09	0.664	0.210
668	1.86	8.58		1.073	11.78		0.210
834	1.74	4.92	175	1.085	3.20	0.784	0.211
834	1.74	7.21		1.076	51.27		0.243
930	1.96	7.66	218	1.087	4.85	-	0.210
930	1.96	9.20		1.064	14.10		0.210
1075	1.90	12.04	258	1.064	31.29	1.144	0.222
1075	1.90	11.10		1.076	71.14		0.210

(1) Potential measured against a saturated calomel electrode.

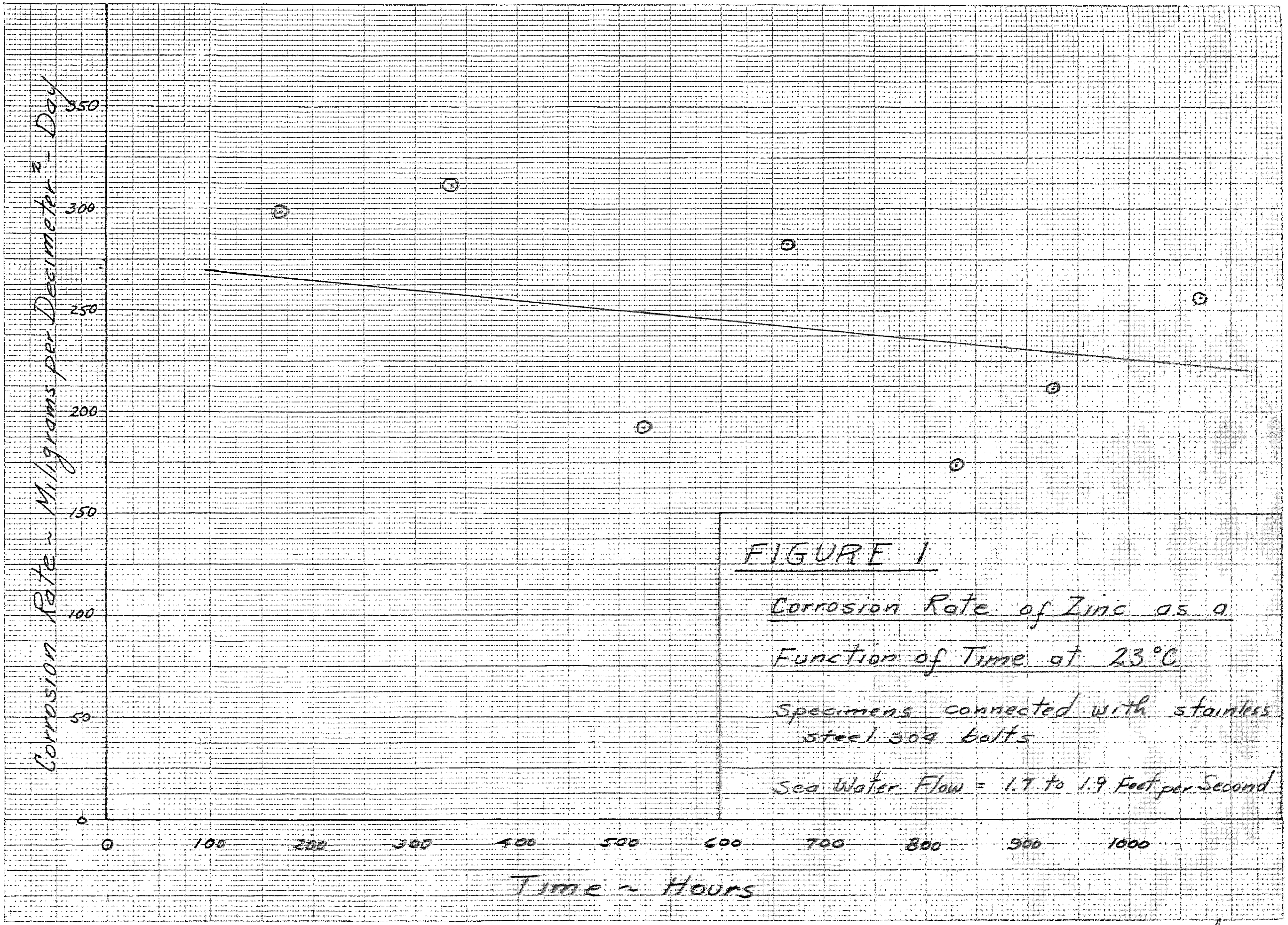

FIGURE 1

Corrosion Rate of Zinc as a Function of Time at 23°C

Specimens connected with stainless steel 304 bolts

Sea Water Flow = 1.7 to 1.9 Feet per Second

Henry Shaw
2/2/62

FIGURE 2

Weight Loss of Zinc as a Function of Time at 23°C

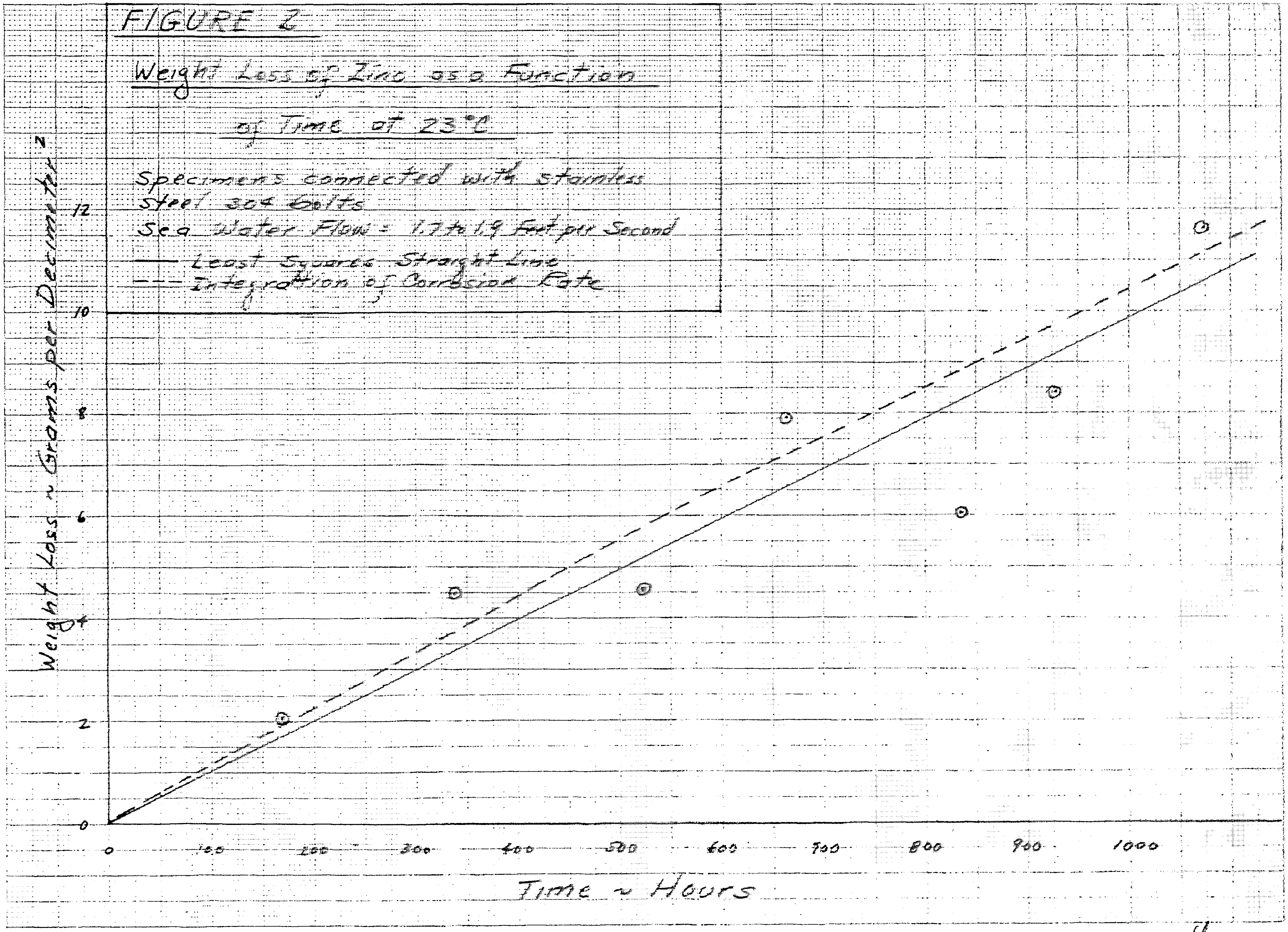

Specimens connected with stainless steel 304 bolts
Sea Water Flow = 1.7 to 1.9 Feet per Second
—— Least Squares Straight Line
- - - Integration of Corrosion Rate

2/2/62

PHOTOGRAPH 5

Corrosion of Zinc as a Function of Time at 23°C - Connected with Stainless Steel 304 Bolts - Flow = 1.7 to 1.9 Feet per Second

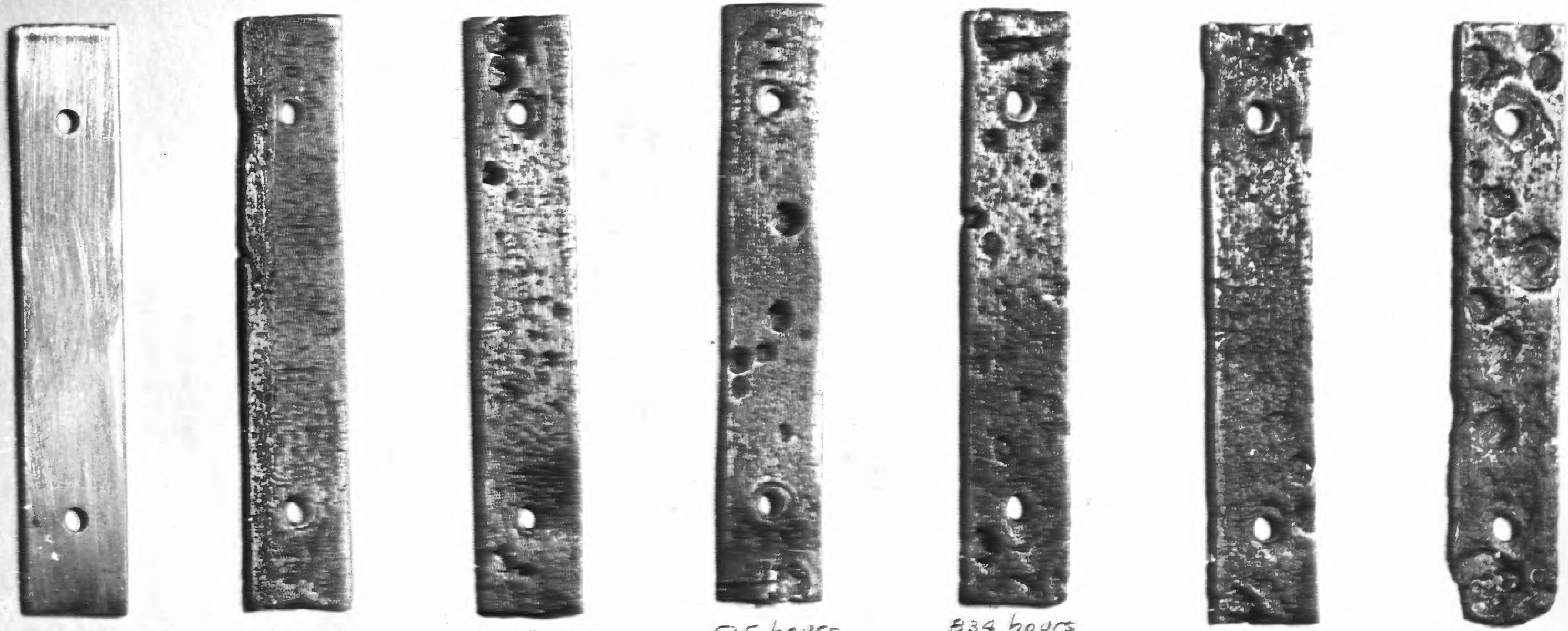

0 hours 168 hours 339 hours 525 hours 834 hours 930 hours 1075 hours

Figure 1 indicates that under flow conditions, there is a definite trend toward a decrease in corrosion rate as a function of exposure time. If this trend is assumed linear, the resulting weight change graph, Figure 2, is a parabola which follows the analytical expression:

$$w = -1.04\text{x}10^{-6}t^2 + 11.45\text{x}10^{-3}t \qquad (3)$$

This curve is seen to approximate a least squares straight line very closely. In general, this curve indicates a film is formed, therefore, reducing the corrosion rate directly as thickness increases.

Equation 3 should not be used for exposures much beyond the time of this experiment nor for exposure shorter than one week.

The average corrosion rate, using the straight line ralationship of Figure 2 is 237 milligrams per square decimeter-day. But, even this number must be qualified by a statement that zinc pitted heavily under these conditions.

Photograph 5 illustrates the degree of pitting as a function of time. The bottom specimen was not exposed and the rest from bottom up represent 168, 339, 525, 834, 930 and 1075 hours subject to a flow of 1.74 to 1.96 feet per second.

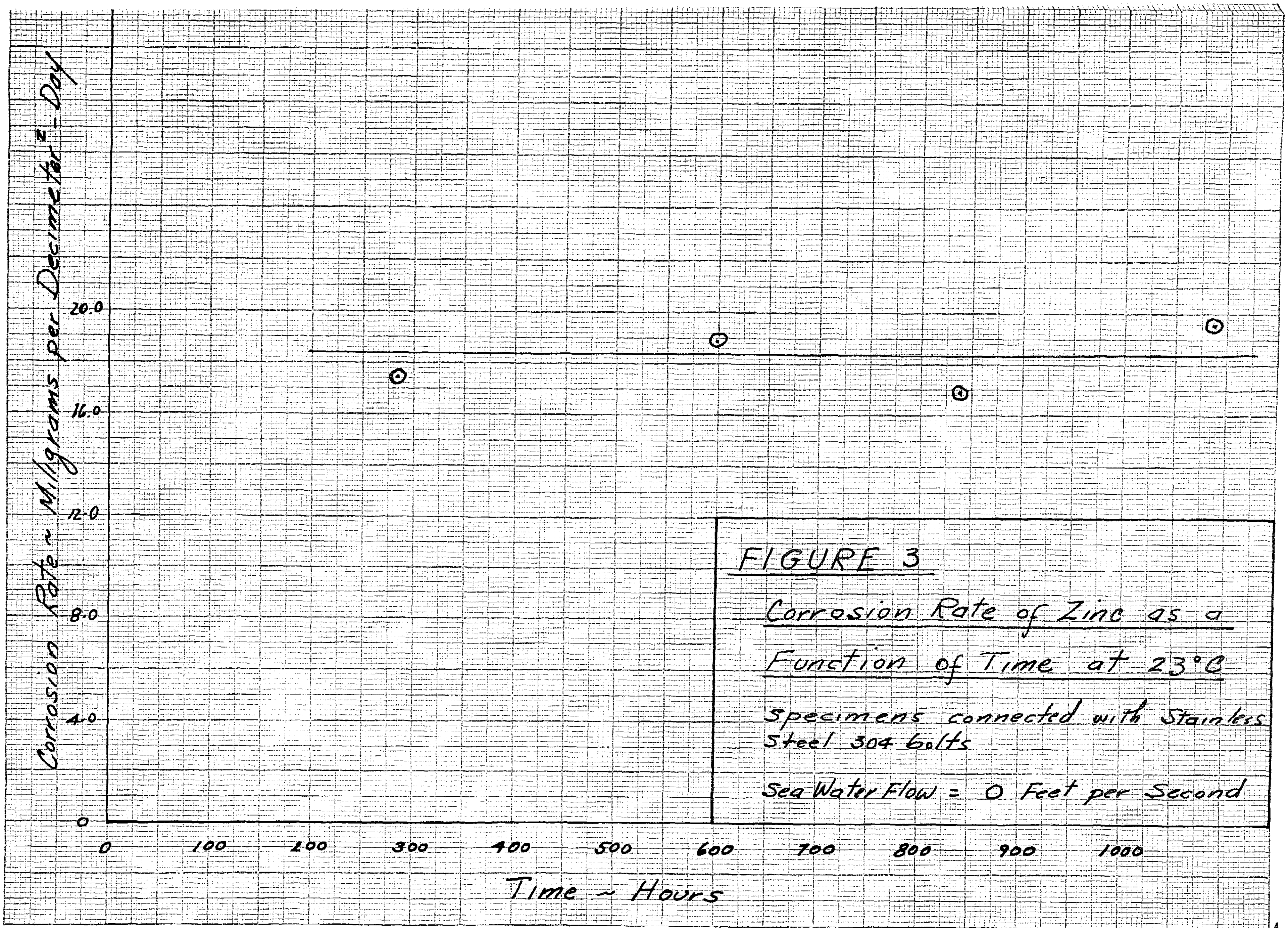

FIGURE 3

Corrosion Rate of Zinc as a Function of Time at 23°C

Specimens connected with Stainless Steel 304 bolts

Sea Water Flow = 0 Feet per Second

4/2/62

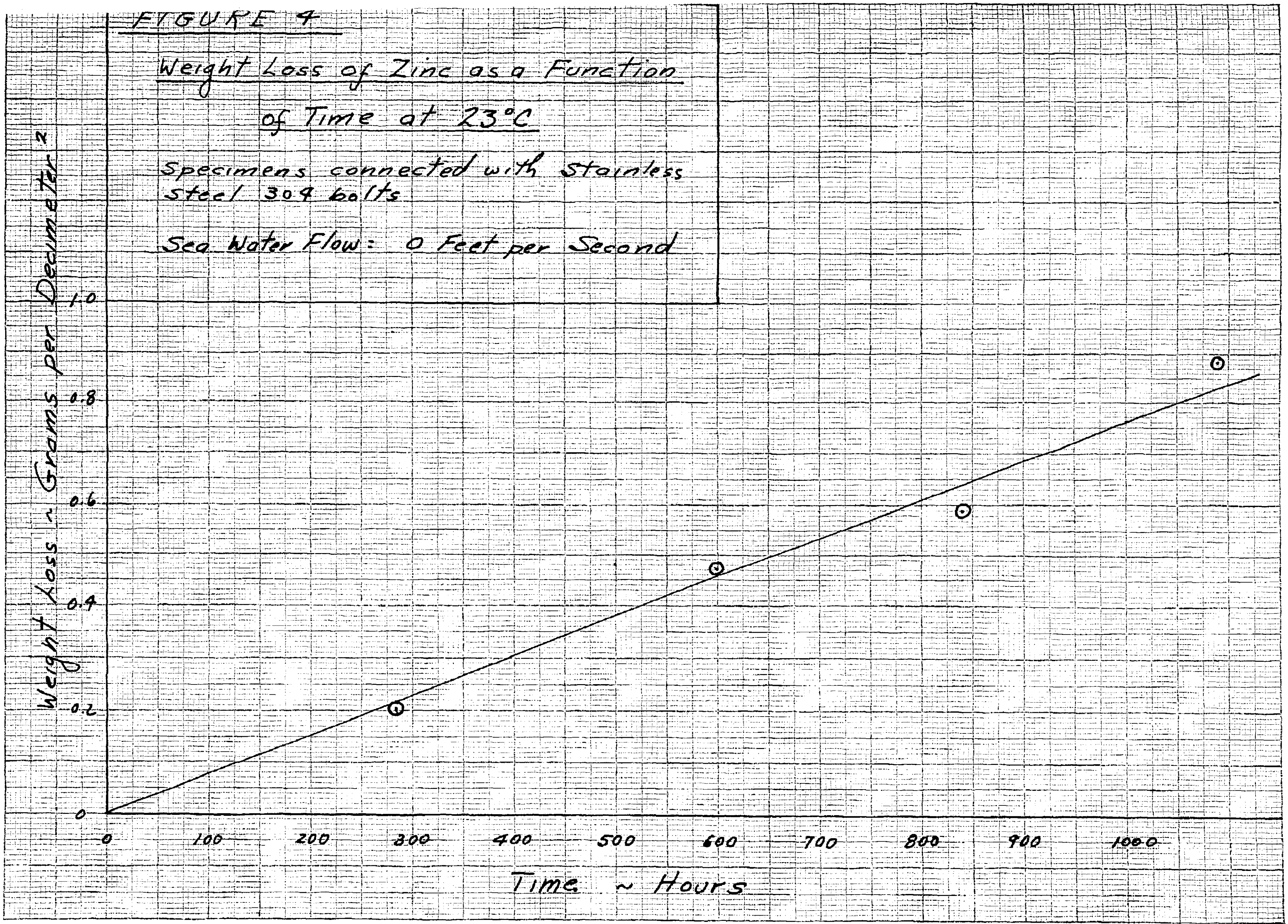

FIGURE 4

Weight Loss of Zinc as a Function of Time at 23°C

Specimens connected with stainless steel 304 bolts

Sea Water Flow: 0 Feet per Second

8/2/62

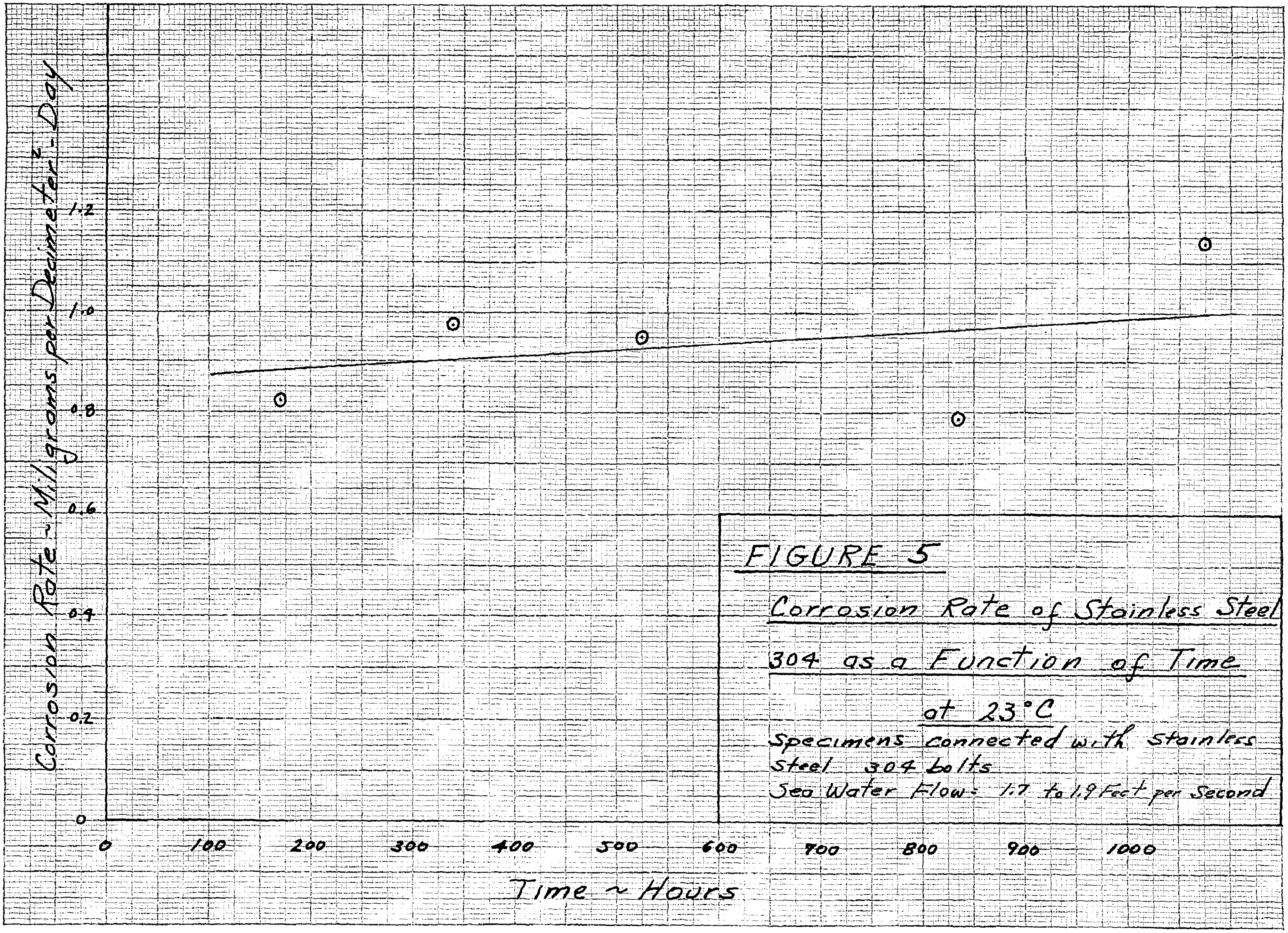

FIGURE 5

Corrosion Rate of Stainless Steel 304 as a Function of Time at 23°C

Specimens connected with stainless steel 304 bolts

Sea Water Flow: 1.7 to 1.9 Feet per Second

Henry Shaw
4-2-62

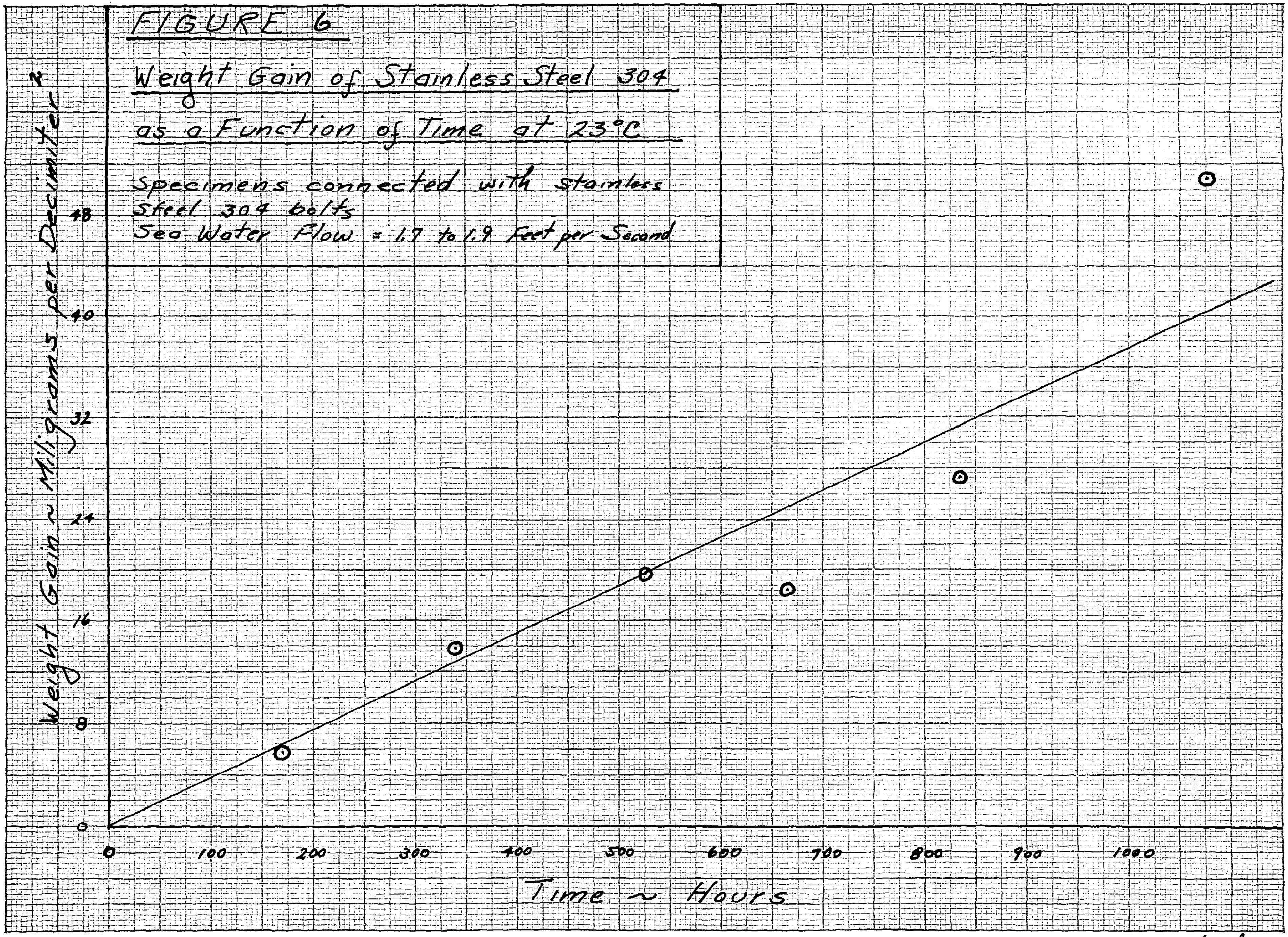

FIGURE 6

Weight Gain of Stainless Steel 304 as a Function of Time at 23°C

Specimens connected with stainless steel 304 bolts
Sea Water Flow = 1.7 to 1.9 Feet per Second

Figure 3 (no flow), on the other hand, indicates a constant rate of corrosion. This is borne out in Figure 4. The mechanism for the no flow condition is, therefore, different from the flow film mechanism. The specimen appearance indicated this by showing no pits, but a dull grey metallic luster. The corrosion rate for zinc connected to stainless steel 304 subject to zero flow is 18.4 milligrams per decimeter square-day.

Figure 5 describes the change of corrosion rate of stainless steel 304 as a function of exposure time.

The analytical expression for weight gain is:

$$w' = 2.71\text{x}10^{-6}t^2 + 3.58\text{x}10^{-2}t \qquad (4)$$

In this case, the trend is toward an increase in rate with time. Equation (4) was not plotted since it falls very closely to the least squares line of Figure 6. It should be brought out that stainless steel always incurred a weight gain as a result of corrosion. Under flow conditions, all stainless specimens came out with a brittle ceramic-like black coat which required hard brushing to remove. The steel surface, after this coat was removed, looked identical to the surface prior to exposure. This coat can possibly be attributed to the circulating iron hydroxides depositing on the stainless steel surface and losing some water molecules to form magnetite.

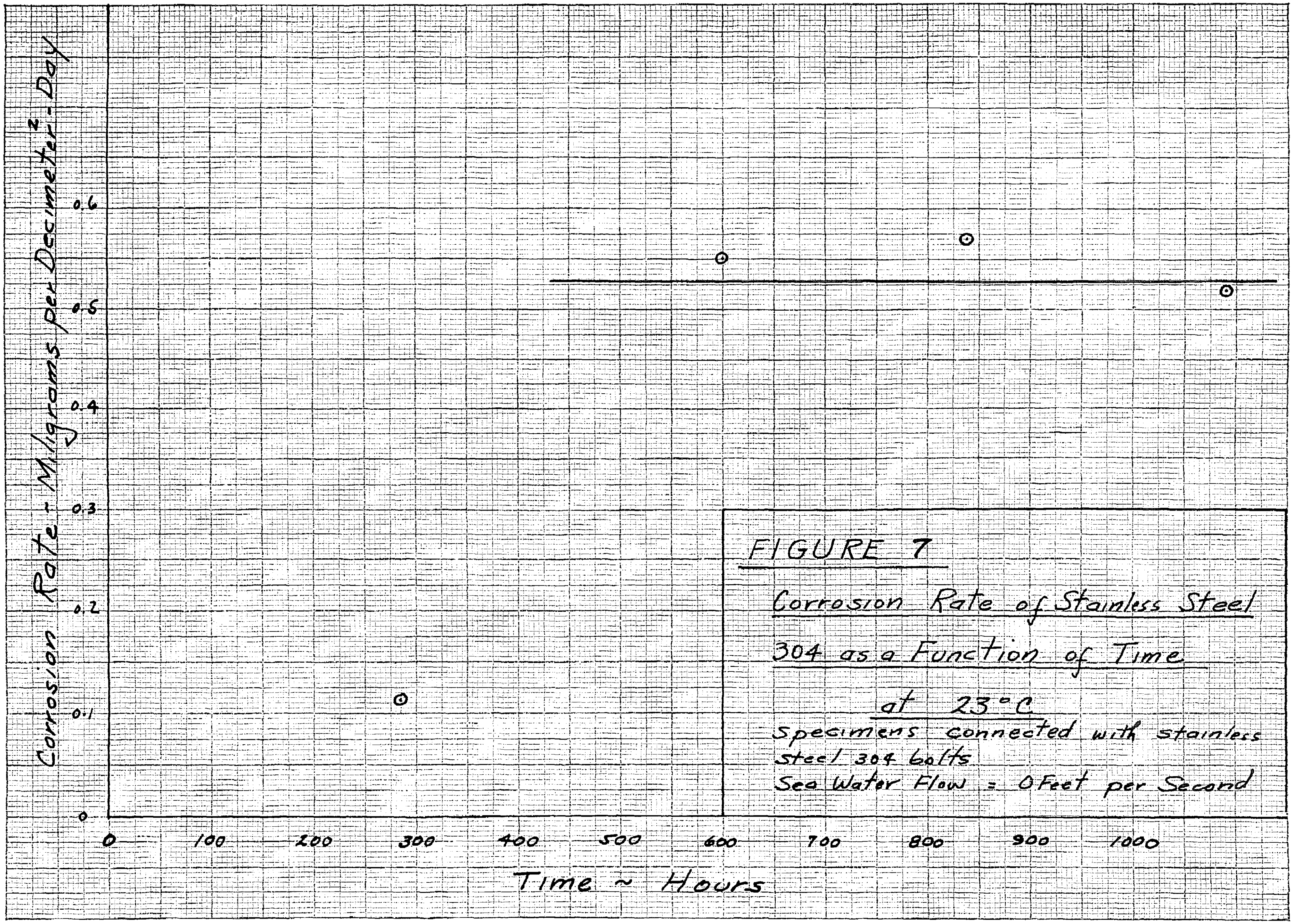

FIGURE 7

Corrosion Rate of Stainless Steel 304 as a Function of Time at 23°C

specimens connected with stainless steel 304 bolts

Sea Water Flow = 0 Feet per Second

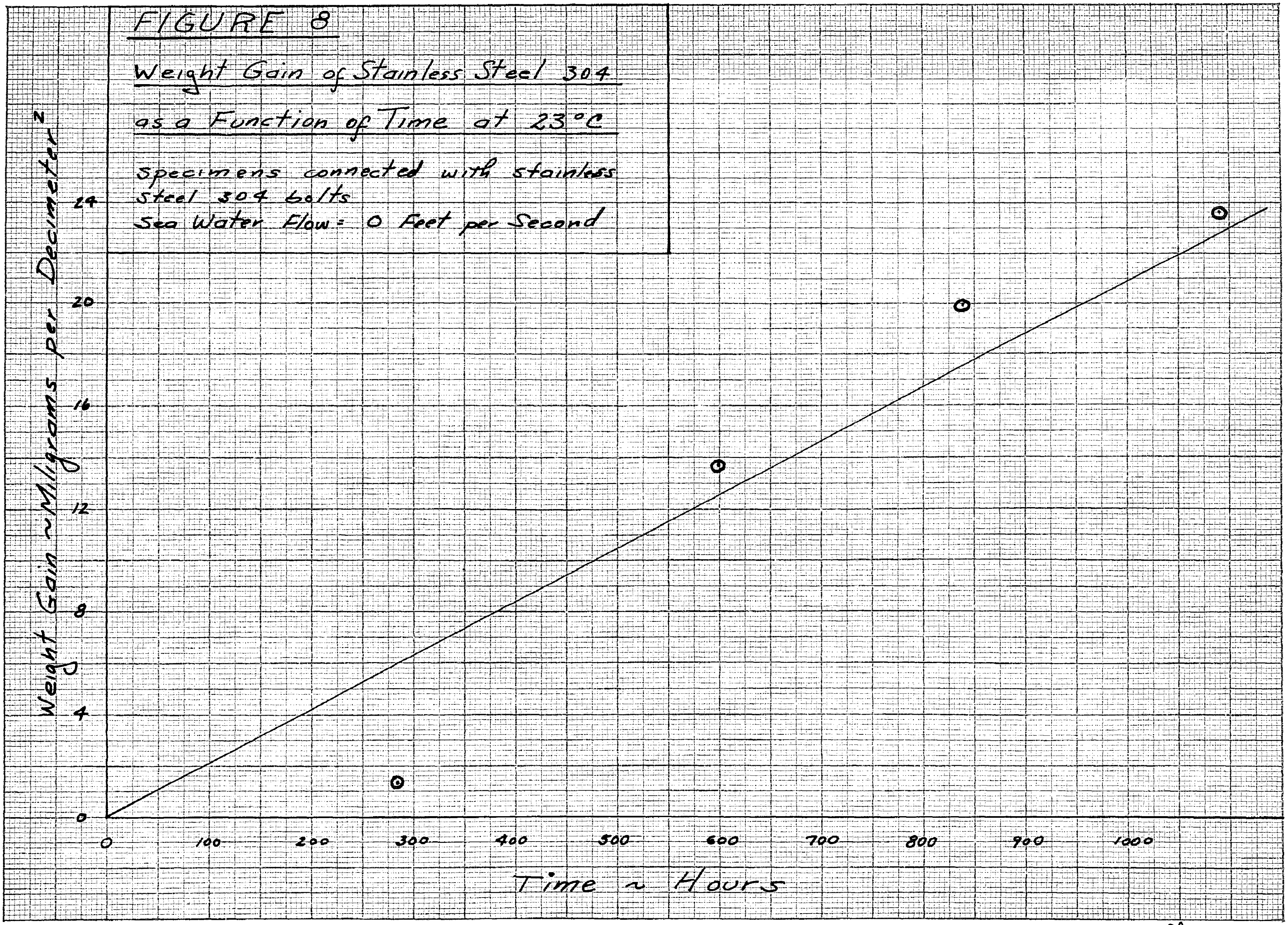

FIGURE 8

Weight Gain of Stainless Steel 304 as a Function of Time at 23°C

Specimens connected with stainless steel 304 bolts
Sea Water Flow = 0 Feet per Second

Henry Shaw

Potter(10) indicates that deposition of red brown rust ($Fe_2O_3 \cdot H_2O$) on cathodic surfaces reduces the availability of oxygen to that surface forming an underlayer of ferrous hydroxide.

$$6Fe(OH)_2 + O_2 \longrightarrow 4H_2O + 2Fe_3O_4 \cdot H_2O$$

$$Fe_3O_4 \cdot H_2O \longrightarrow H_2O + Fe_3O_4 \quad \text{(black magnetite)}$$

The net effect of this on the corrosion of the stainless is not known. The above speculations are just qualitative in nature and are not based on any chemical analysis of the black coating.

The corrosion of stainless steel 304 under no flow condition is plotted in Figures 7 and 8. The corrosion rate is 0.53 milligram per square decimeter day as opposed to 0.90 mdd. for the stainless subject to flow. The appearance of the stainless steel 304 specimen was not altered by corrosion from their appearance prior to corroding.

Velocity Effect on "Sea Water Connection"

The effect that the sea water itself has on conducting the corrosion current between the zinc and stainless steel was determined. This factor is of interest since it indicates that when the specimens are close enough to each other a direct metallic connection is not necessary to form a galvanic couple.

TABLE 5

The Sea Water Corrosion of Zinc-Stainless Steel 304 Specimens Coupled with Insulated Bolts at 23°C.

		Zinc			Stainless Steel		
Time hrs	Flow Rate Ft/sec	Weight Loss g/dm^2	Rate mdd	Potential$^{(1)}$ volts	Weight Gain mg/dm^2	Rate mdd	Potential$^{(1)}$ volts
Static							
283	0	0.088	10.34	1.056	15.27	1.03	0.219
283	0	0.157		1.075	9.00		0.216
598	0	0.333	16.74	1.081	6.06	0.526	0.230
598	0	0.500		1.069	20.04		0.297
839	0	0.354	14.76	1.073	10.75	0.416	0.260
839	0	0.678		1.075	18.34		0.272
1090	0	0.910	21.16	1.085	18.50	0.410	0.300
1090	0	1.011		1.059	18.77		0.271
Dynamic							
168	1.74	1.93	214	1.063	19.37	1.58	0.265
168	1.74	1.06		1.080	2.75		0.273
339	1.86	4.56	311	1.062	13.38	0.972	0.219
339	1.86	4.24		1.076	14.08		0.217
525	1.76	1.26	252	1.062	11.85	0.771	0.229
525	1.76	9.74		1.071	21.89		0.220
665	1.94	3.01	82	1.067	9.19		0.217
665	1.94	1.53		1.082	6.21		0.239
834	1.30	8.34	240	1.093	33.42	0.806	0.221
834	1.30	Very Large		1.079	22.67		0.225
1075	1.32	7.47	136	1.064	8.12	0.054	0.230
1075	1.32	4.72		1.064	68.39		0.230

(1) Potential Measured against a saturated Calomel Electrode.

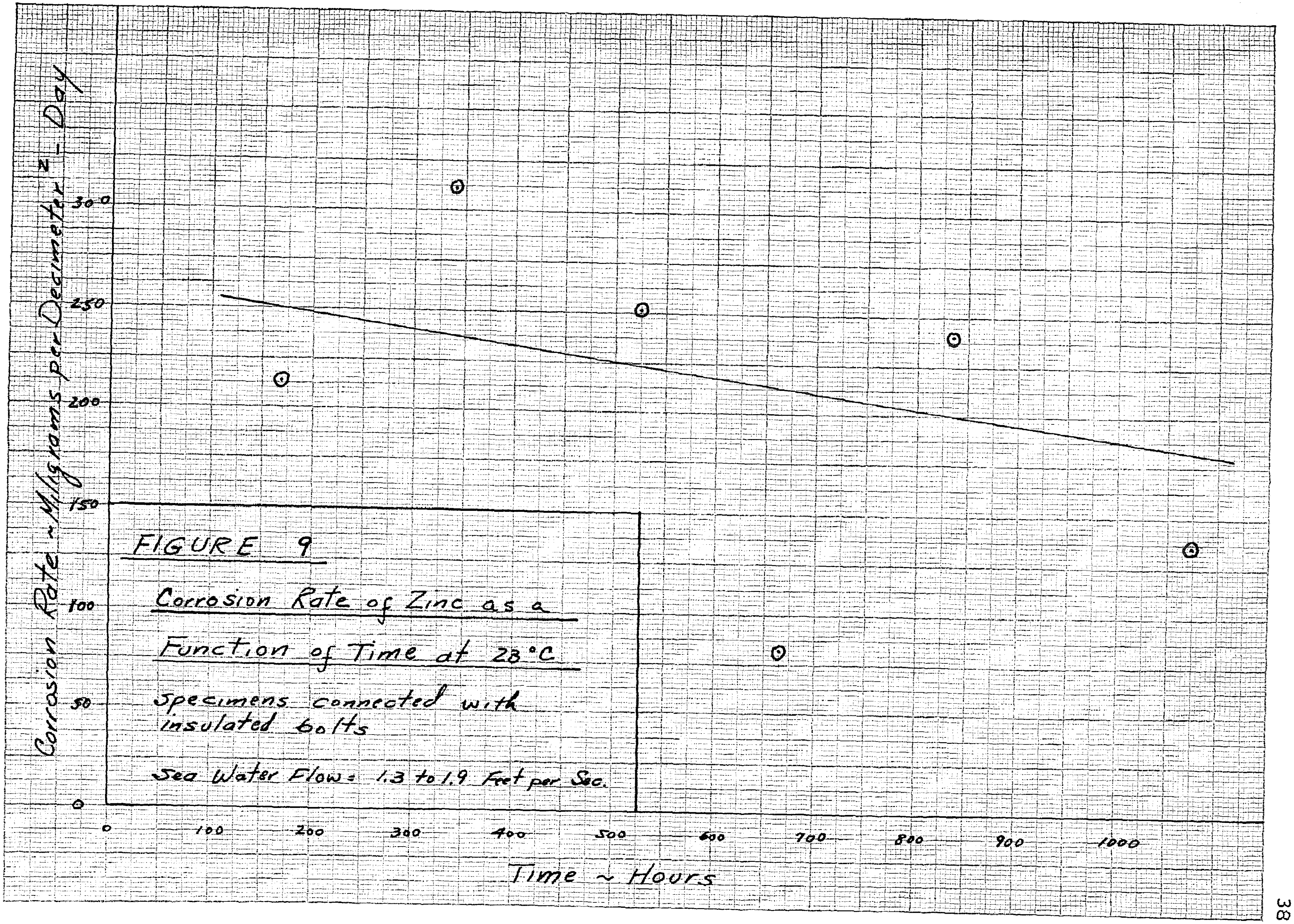

FIGURE 9

Corrosion Rate of Zinc as a Function of Time at 28°C

Specimens connected with insulated bolts

Sea Water Flow = 1.3 to 1.9 Feet per Sec.

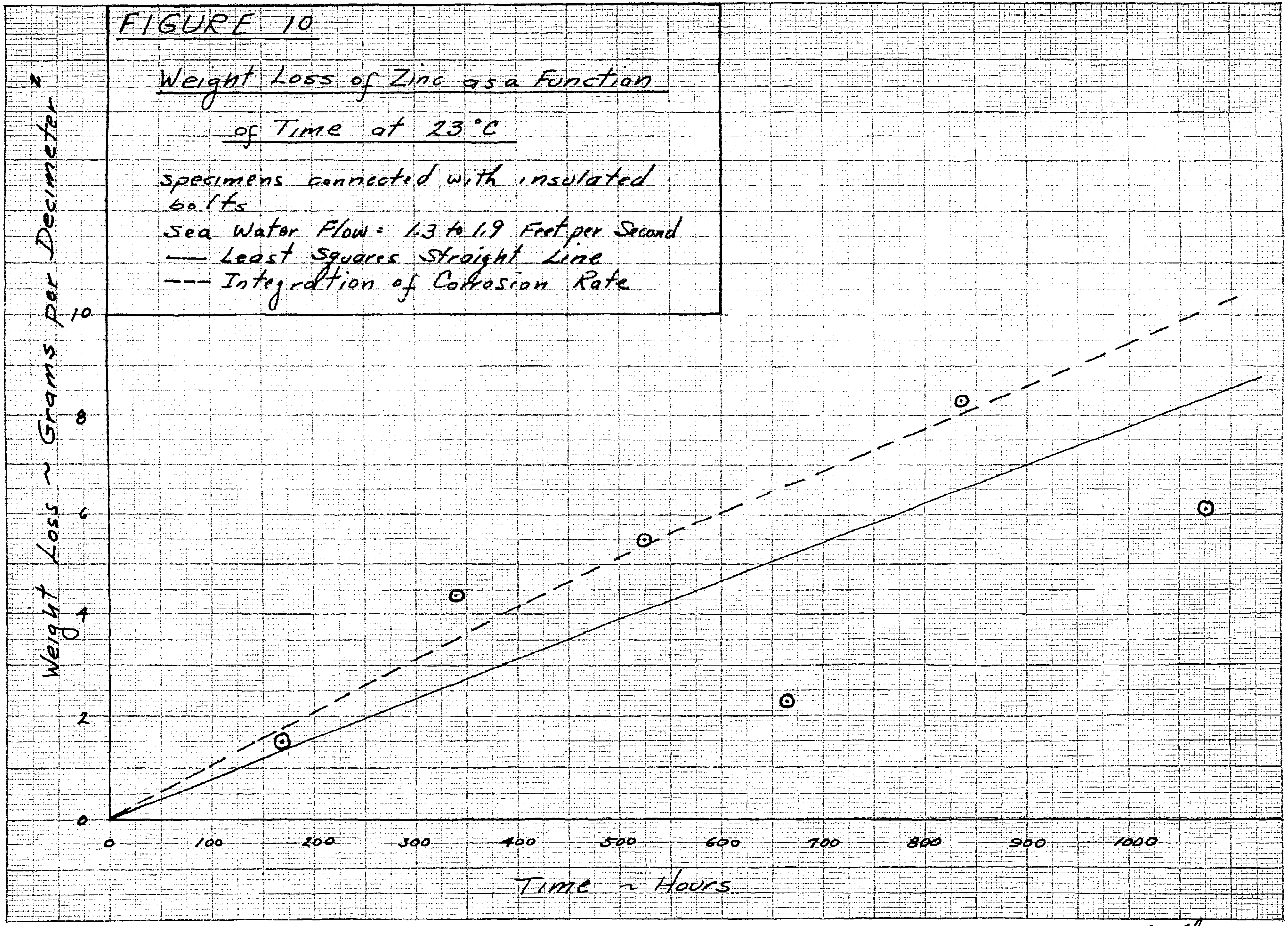

FIGURE 10

Weight Loss of Zinc as a Function of Time at 23°C

PHOTOGRAPH 6

Corrosion of Zinc as a Function of Time at 23°C - Connected with Insulated Bolts - Flow = 1.3 to 1.9 Feet per Second.

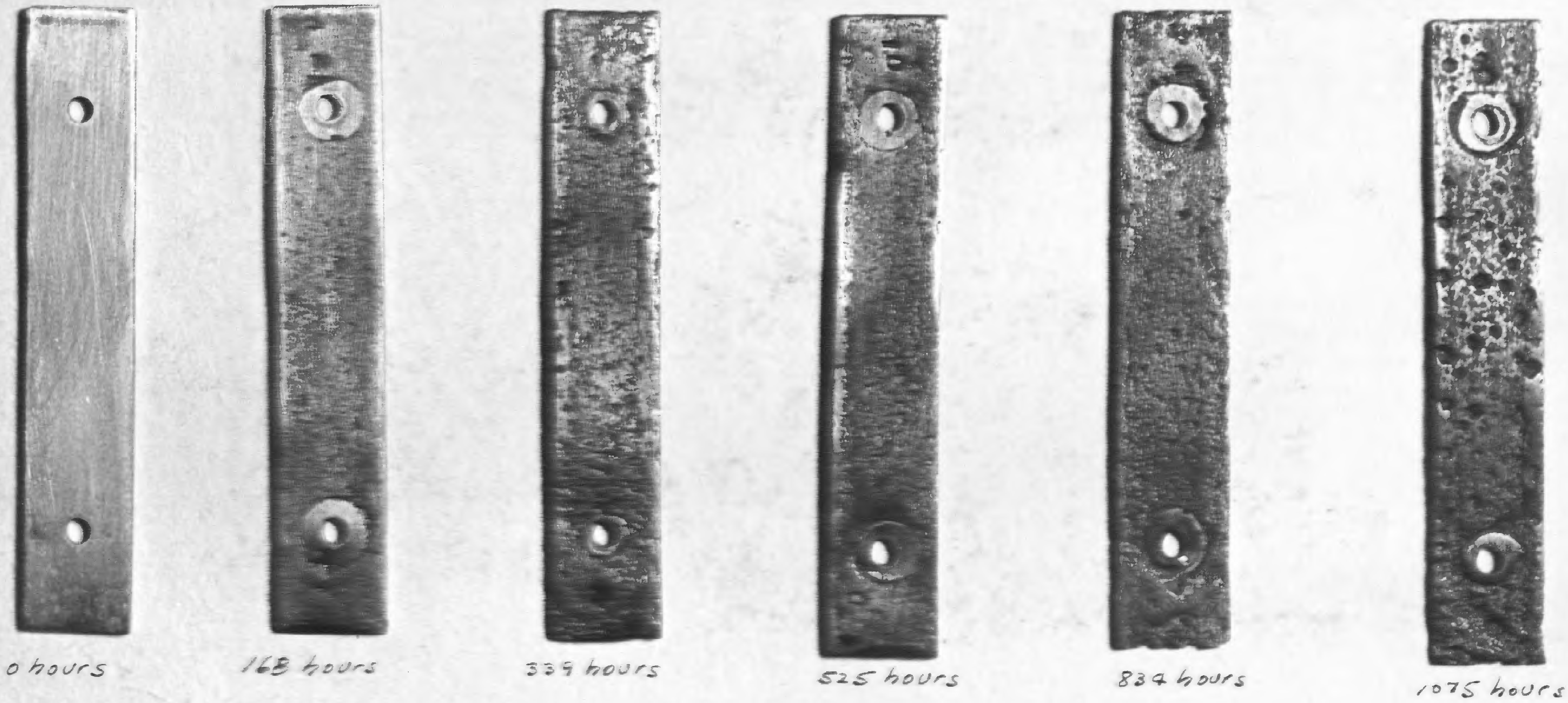

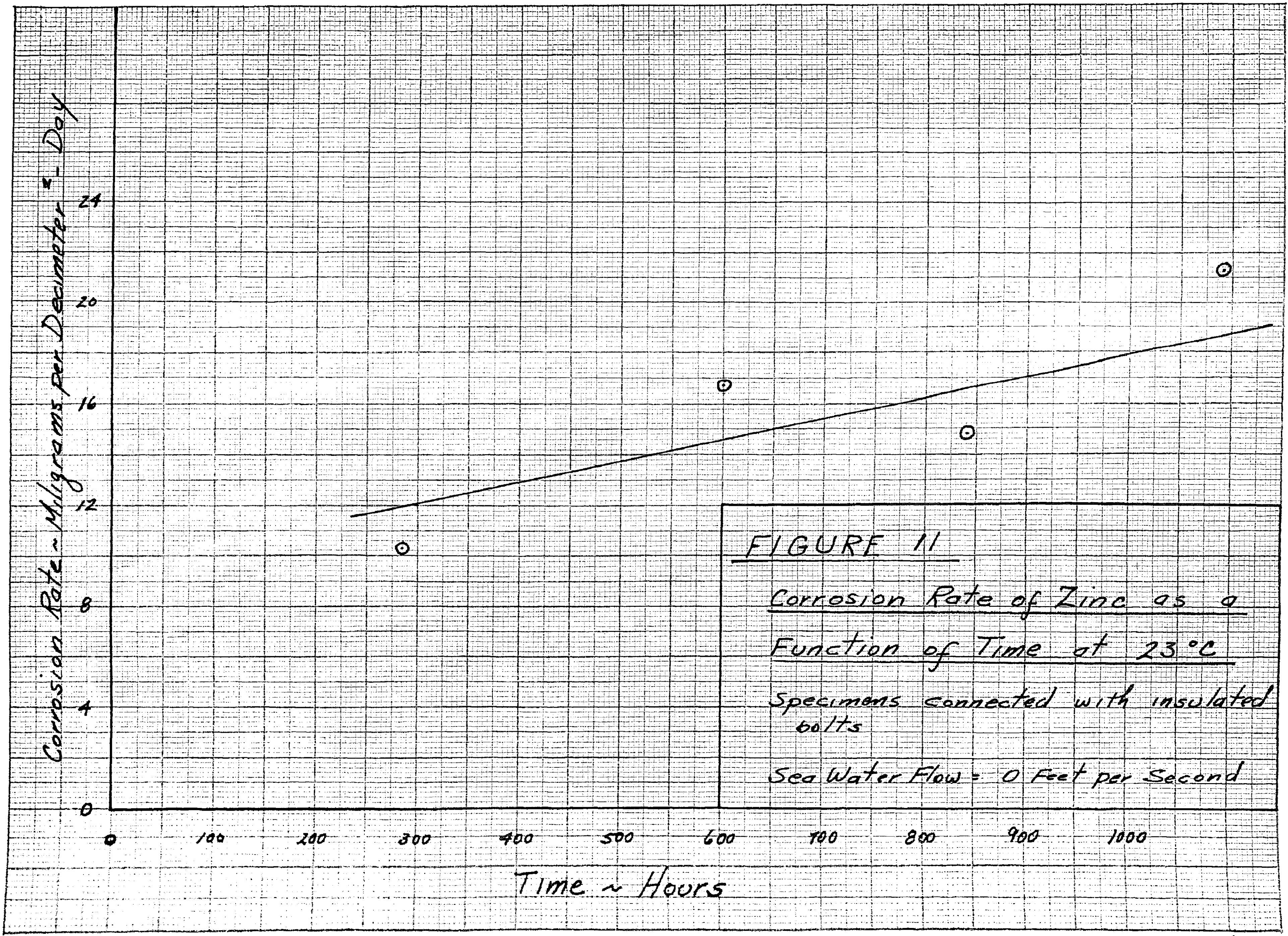

FIGURE 11

Corrosion Rate of Zinc as a Function of Time at 23°C

Specimens connected with insulated bolts

Sea Water Flow = 0 Feet per Second

Hey Shaw
6/2/62

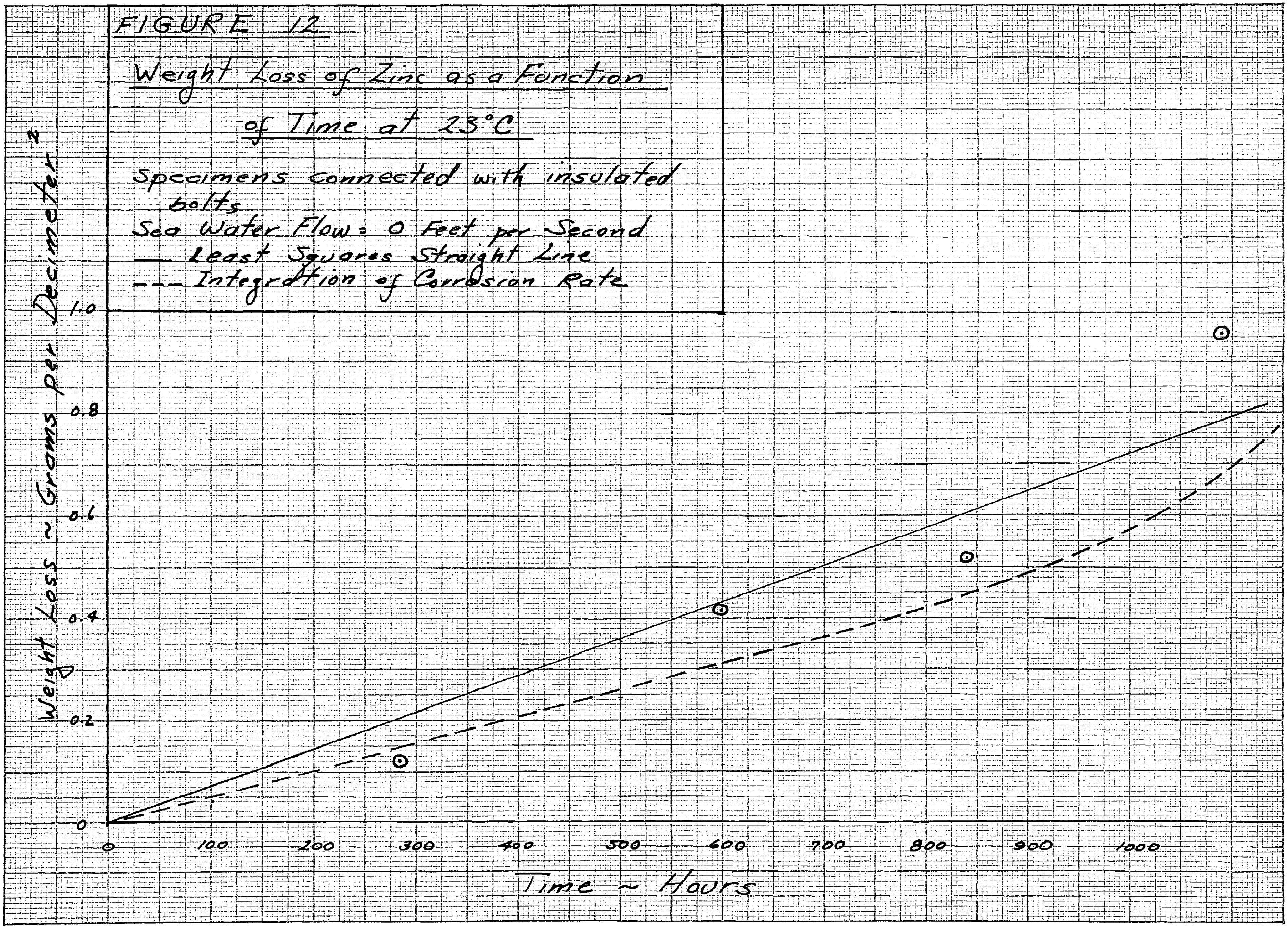

FIGURE 12

Weight Loss of Zinc as a Function of Time at 23°C

Specimens connected with insulated bolts

Sea Water Flow = 0 Feet per Second

— Least Squares Straight Line

--- Integration of Corrosion Rate

Figure 9 is a plot of corrosion rate as a function of time for the galvanic couple connected with sea water. There is considerable scatter in this phase mostly because the specimen assembly procedure did not allow for perfect insulation of the stainless steel bolts which were used for the assembly. The analytic function which seemed to fit the weight gain data best is:

$$w = -1.56 \times 10^{-6} t^2 + 10.9 \times 10^{-3} t \qquad (5)$$

The curve of equation (5) is compared to the least squares straight line of Figure 10. The corrosion mechanism suggested seems to parallel the one described for zinc specimens connected with stainless steel. The differences in pitting can be seen in photograph 6. The zinc specimens were exposed for 0, 168, 339, 525, 834 and 1075 hours. Oxygen concentration cells were formed around the tygon separator and can be clearly seen in Photograph 6.

The average corrosion rate of zinc for the sea water connected couple is 187 milligrams per square decimeter-day.

The no flow experiment for this part indicated a corrosion rate which increased with time, Figure 11. Although this seems to indicate a mechanism which differs radically from those described previously, it is still reported here with the added precaution that it is based on only four experimental points. The equation which results is concave upwards and can be written as:

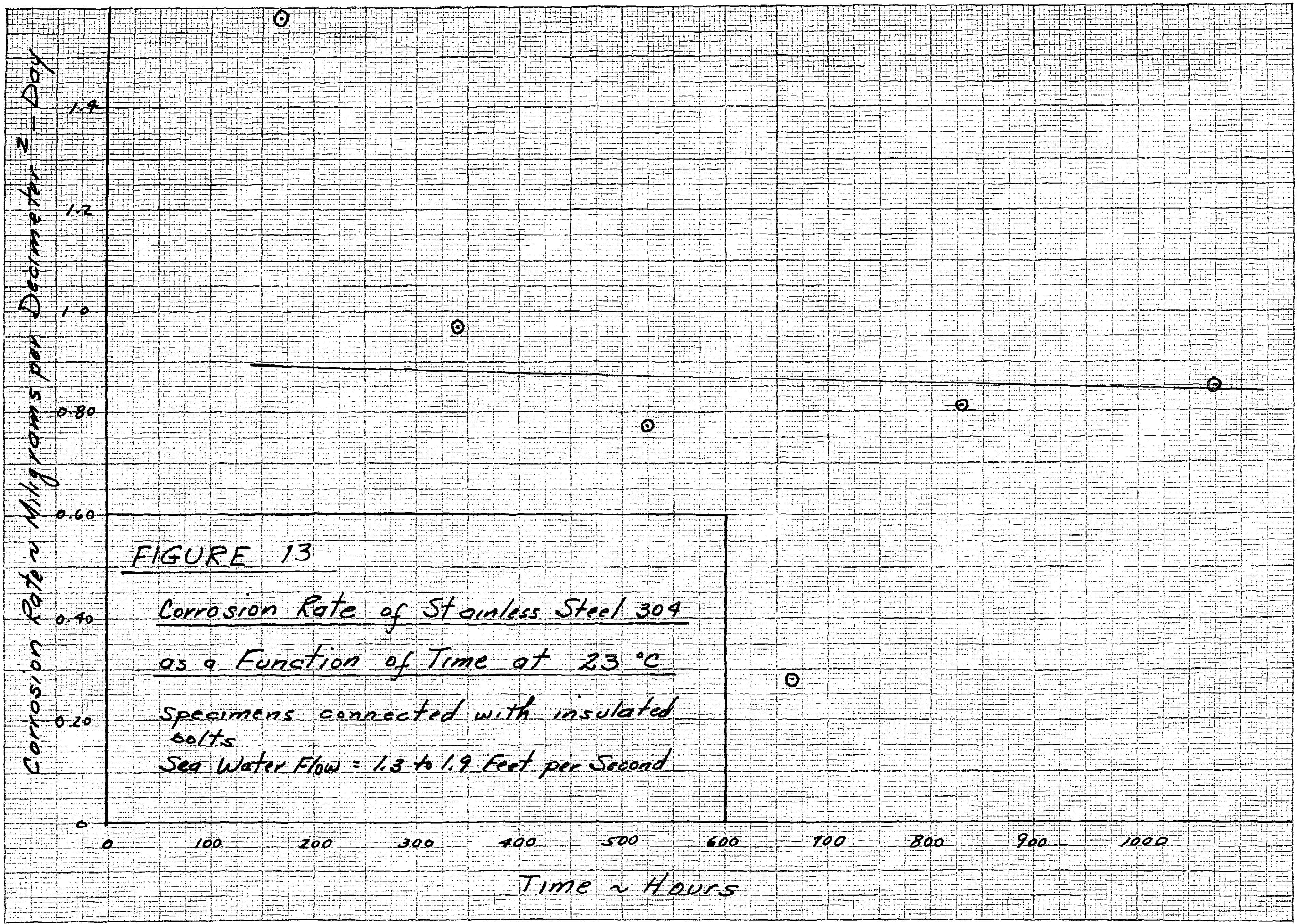

FIGURE 13

Corrosion Rate of Stainless Steel 304 as a Function of Time at 23 °C

Specimens connected with insulated bolts

Sea Water Flow = 1.3 to 1.9 Feet per Second

Henry Shaw

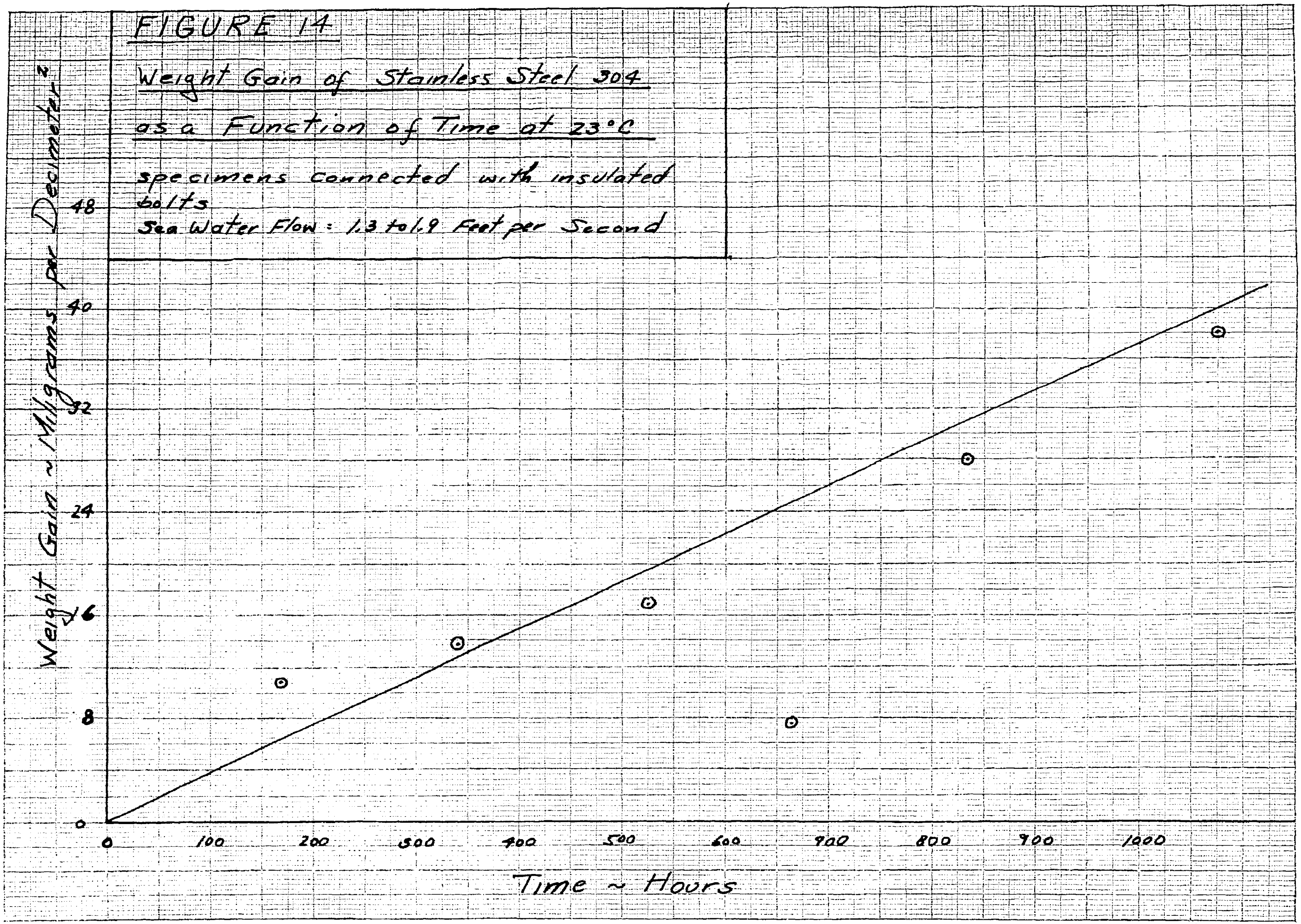

FIGURE 14

Weight Gain of Stainless Steel 304 as a Function of Time at 23°C

specimens connected with insulated bolts
Sea Water Flow: 1.3 to 1.9 Feet per Second

4-2-62

$$w = 1.77\times10^{-7}t^2 + 3.96\times10^{-4}t \qquad (6)$$

The corresponding corrosion rate, based on the least squares straight line of Figure 12, is 17.7 milligrams per square decimeter-day. This indicates a very slight difference between this experiment and the static experiments with stainless conduction. The appearance of the static zinc specimens was identical with the ones described in the previous section.

The stainless steel 304 behavior in this phase is analogous to the stainless behavior in the metallically connected couples. Figure 13 indicates considerable scatter which, as indicated above, is believed due to non-uniform resistance between the zinc and stainless members of the couple causing different current density effects. Although there is a strong indication that this curve is not linear, a line was drawn as an approximation for the duration of the test, in order to keep the data analysis consistent. Figure 14 bears out that the straight line approximation is representative of the data. The appearance of the stainless steel specimens was identical to that reported in the previous section and the corrosion rate is very similar at 0.94 milligram per square decimeter-day.

Figures 15 and 16 represent the data for the zero flow condition. This data was also identical to the ones reported

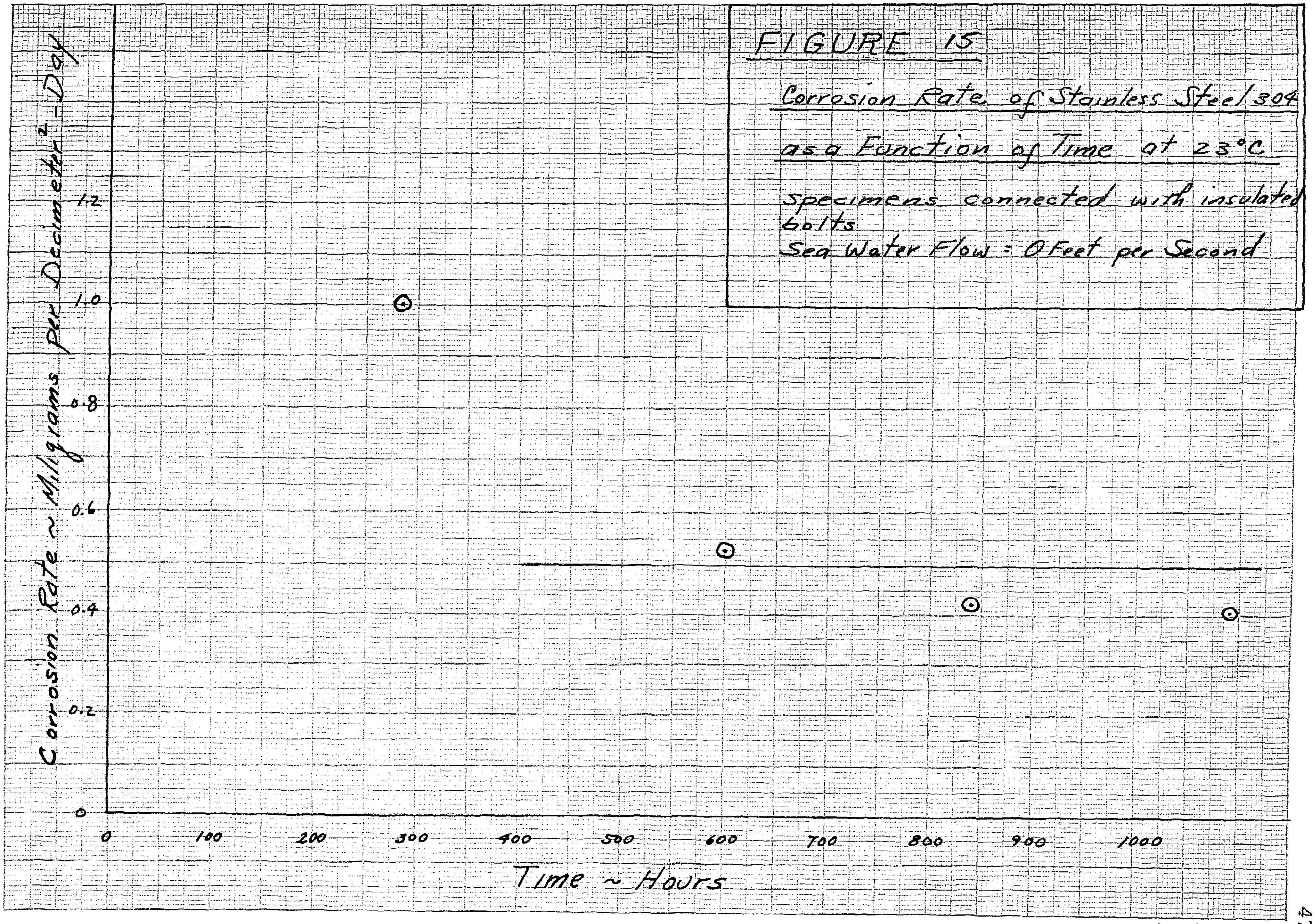

FIGURE 15

Corrosion Rate of Stainless Steel 304 as a Function of Time at 23°C

specimens connected with insulated bolts

Sea Water Flow = 0 Feet per Second

4-2-62

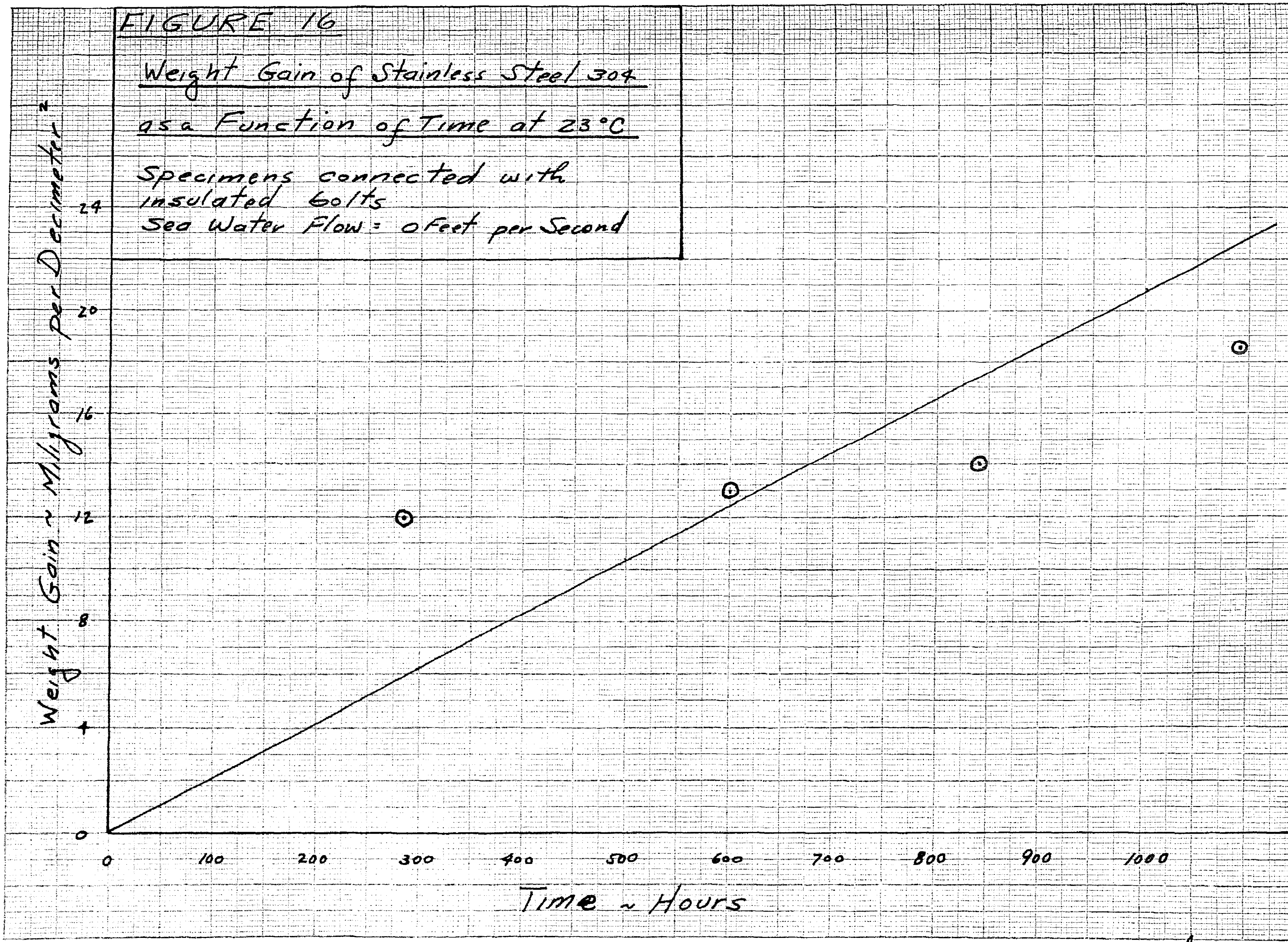

FIGURE 16

Weight Gain of Stainless Steel 304 as a Function of Time at 23°C

Specimens connected with insulated bolts
Sea Water Flow = 0 Feet per Second

Henry Shaw
4-2-62

in the previous section and corresponds to 0.50 milligrams per square decimeter-day.

Veolcity Effect on the Metals Themselves

Table 6 tabulates the data for zinc exposed to sea water in the absence of stainless steel 304.

TABLE 6

The Sea Water Corrosion of Zinc at 23°C

Time hrs	Flow Rate ft/sec	Weight Loss mg/dm^2	Corrosion Rate mdd
	Static		
193	0	35.8	4.9
193	0	42.5	
361	0	80.7	4.7
361	0	59.2	
642	0	97.1	3.3
642	0	76.9	
743	0	125.0	3.5
743	0	89.6	
910	0	107.0	2.7
910	0	97.2	
1099	0	146.2	2.6
1099	0	95.8	
	Dynamic		
73	1.63	652	191.0
73	1.63	510	
168	1.58	1450	177.0
168	1.58	1030	
365	1.46	2360	97.5
365	1.46	1590	
557	1.58	1540	66.0
557	1.58	1510	
809	1.39	3280	82.4
809	1.39	2250	
986	1.49	2650	55.0
986	1.49	1860	

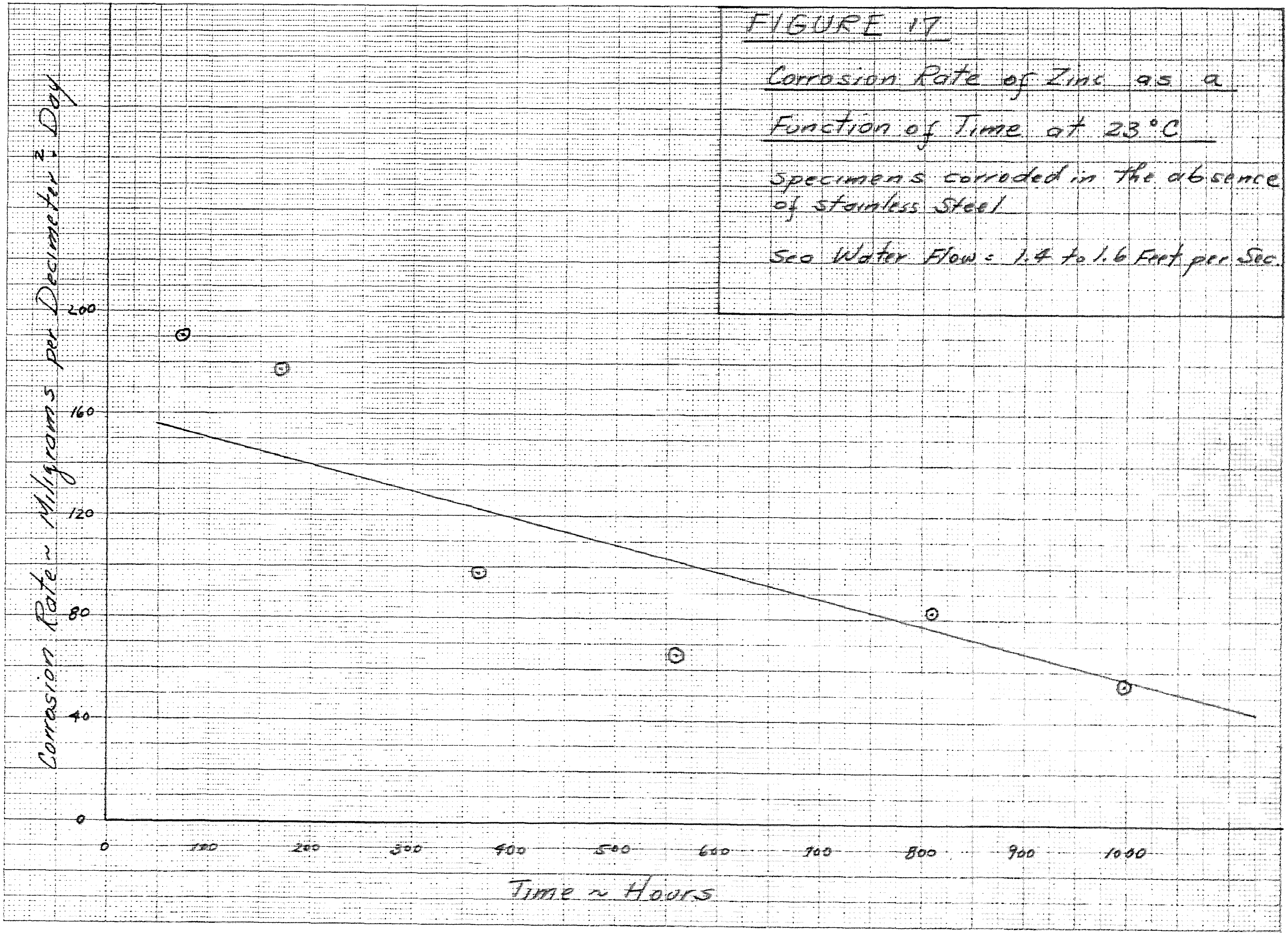

FIGURE 17

Corrosion Rate of Zinc as a Function of Time at 23°C

Specimens corroded in the absence of stainless Steel

Sea Water Flow = 1.4 to 1.6 Feet per Sec.

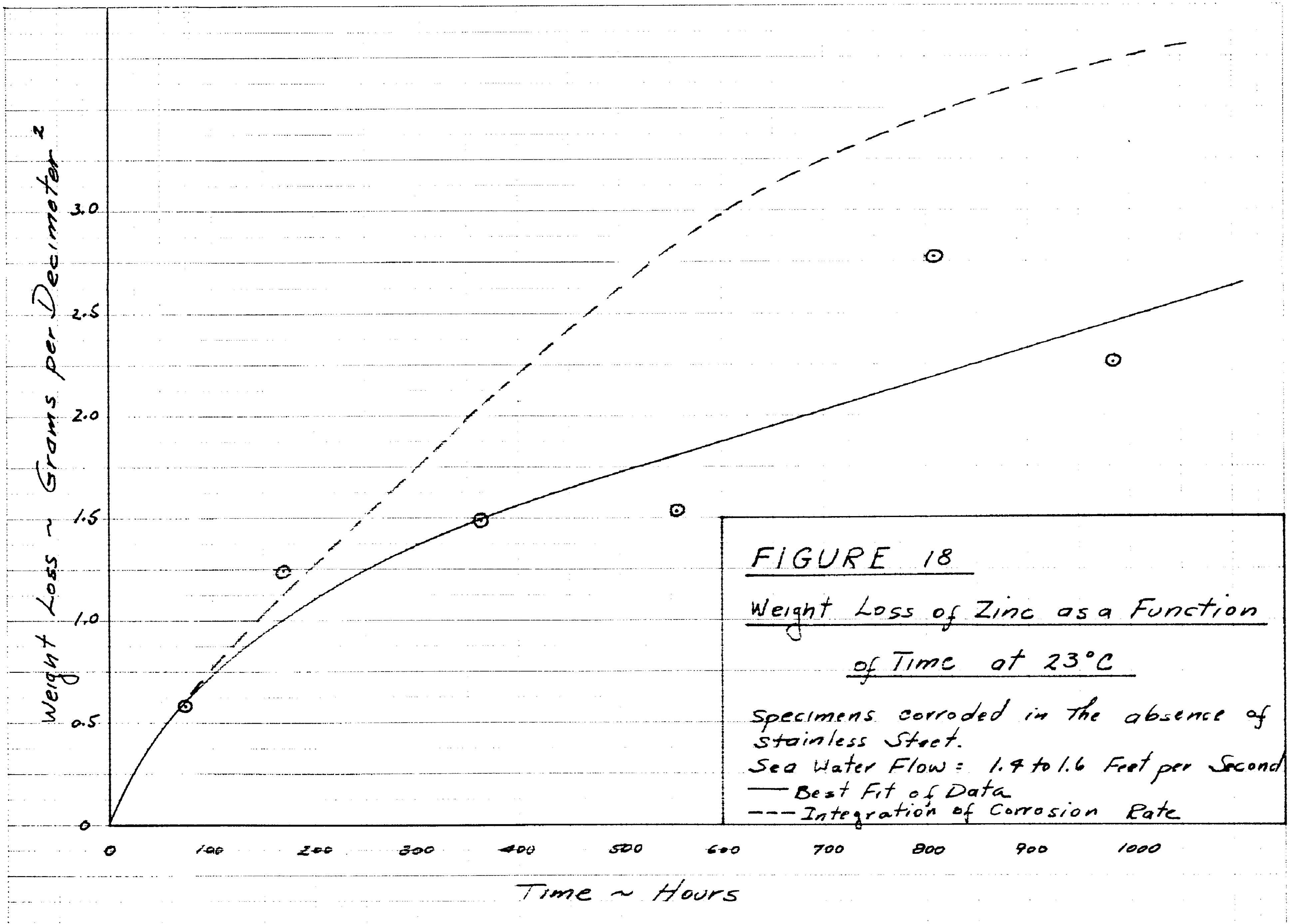

FIGURE 18

Weight Loss of Zinc as a Function of Time at 23°C

Specimens corroded in the absence of stainless Steel.
Sea Water Flow: 1.4 to 1.6 Feet per Second
— Best Fit of Data
--- Integration of Corrosion Rate

Henry Shaw

PHOTOGRAPH 7

Corrosion of Zinc as a Function of Time at 23°C - Stainless Steel 304 Absent - Flow = 1.4 to 1.6 Feet per Second

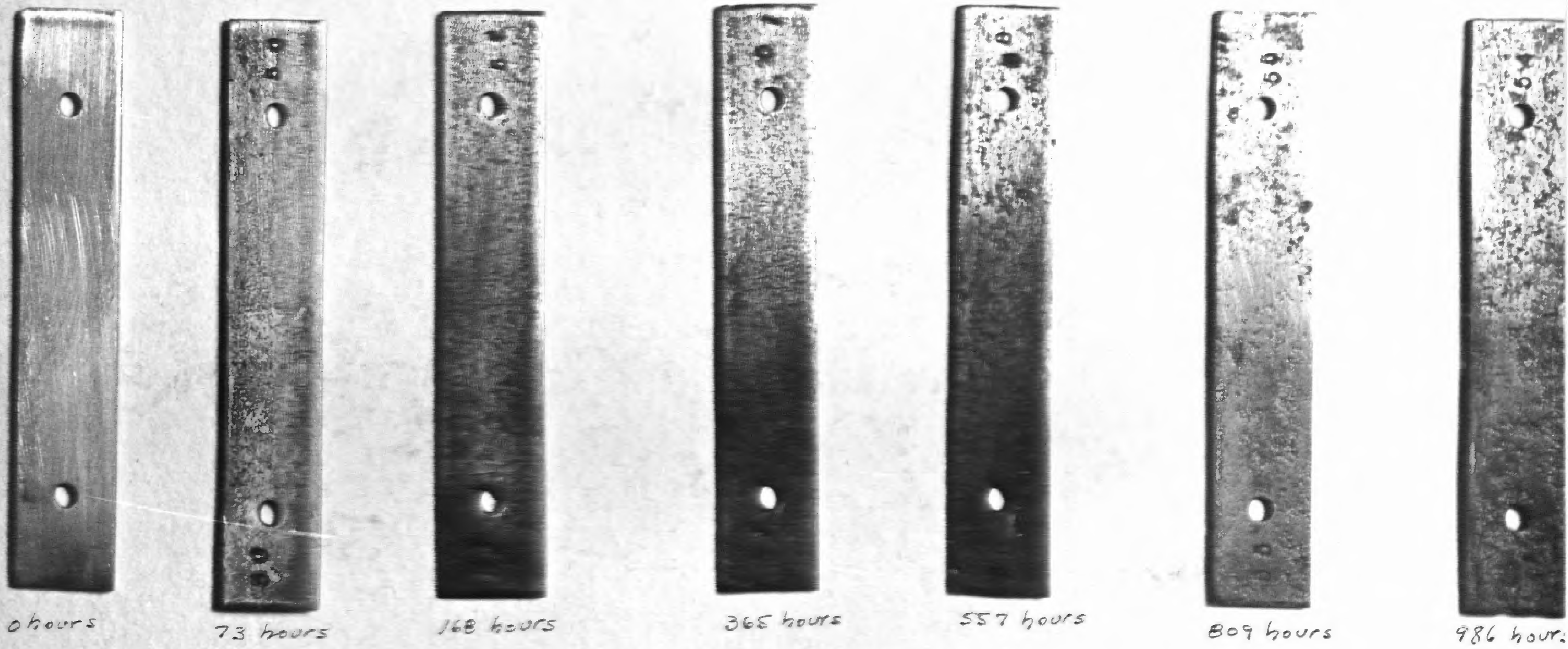

Figure 17 indicates in general that zinc corrosion follows a similar mechanism of corrosion whether coupled or not. On further evaluation of the data, as in Figure 18, the corrosion of zinc seems to follow a parabolic function much in the same sense that Evans(3) attributes to a protective film. In this case, the analytical function derived from the rate function is:

$$w = -2.21\times10^{-6}t^2 + 6.67\times10^{-3}t \tag{7}$$

Equation (7) does not fit the data except for very short exposures. The visual appearance of these specimens is illustrated in Photograph 7. The corrosion times represented are 0, 73, 168, 365, 557, 809 and 986 hours. As can be seen, these specimens were pitted very lightly. The corrosion rate which was used to represent this aspect of the work was based on the slope of the "best fit curve" between 500 and 1000 hours. This value is 38 milligrams per square decimeter-day.

The corrosion rate and weight loss data for zero flow were plotted in Figures 19 and 20. The same type of correlation that applied for the flow condition seemed to apply in the no flow condition. The analytic function resulting from the corrosion rate curve was:

$$w' = -6.25\times10^{-5}t^2 + 0.233t \tag{8}$$

This equation was found to apply only to the initial corrosion. The appearance of these specimens indicated only

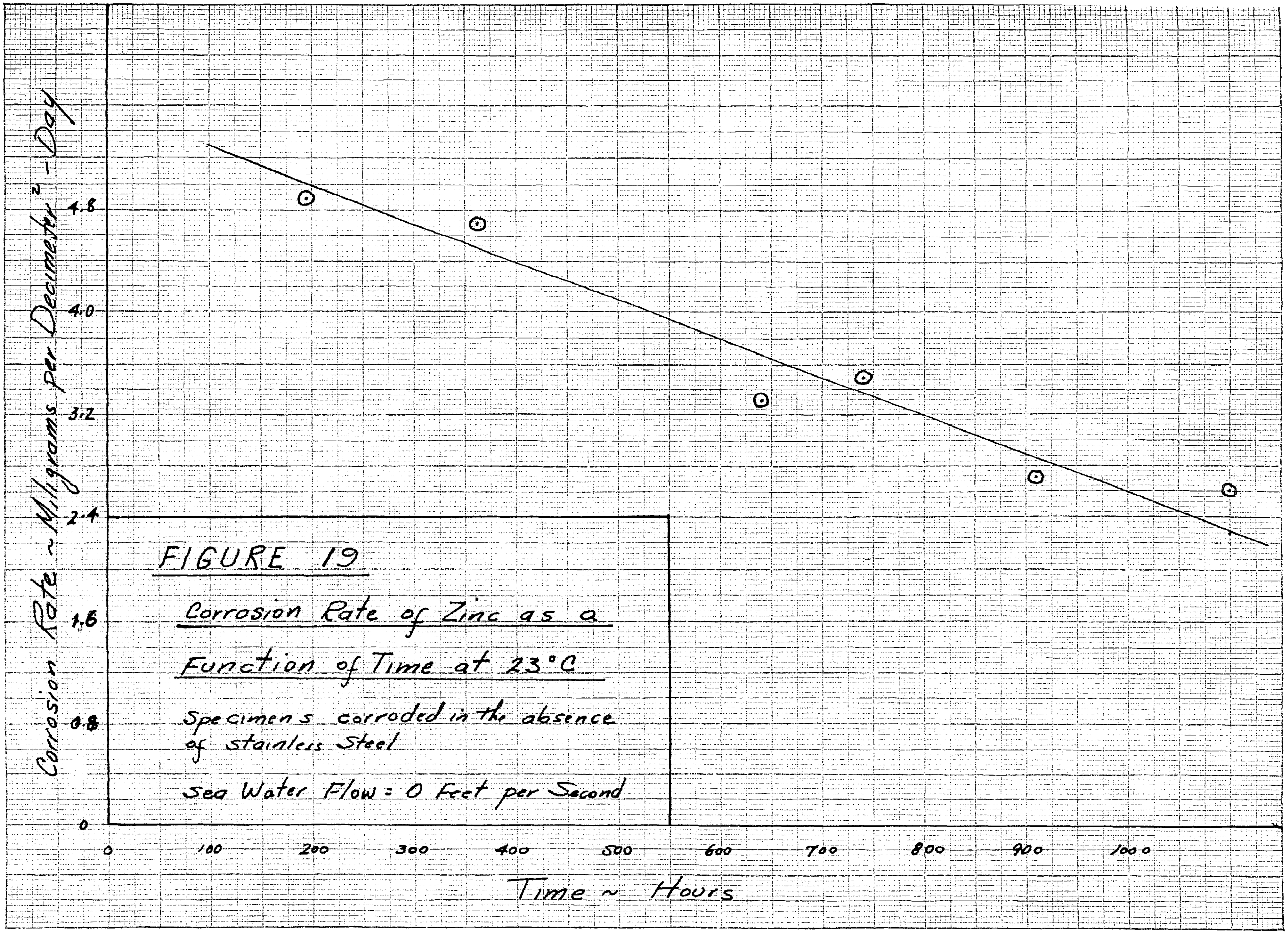

FIGURE 19

Corrosion Rate of Zinc as a Function of Time at 23°C

Specimens corroded in the absence of stainless Steel

Sea Water Flow = 0 Feet per Second

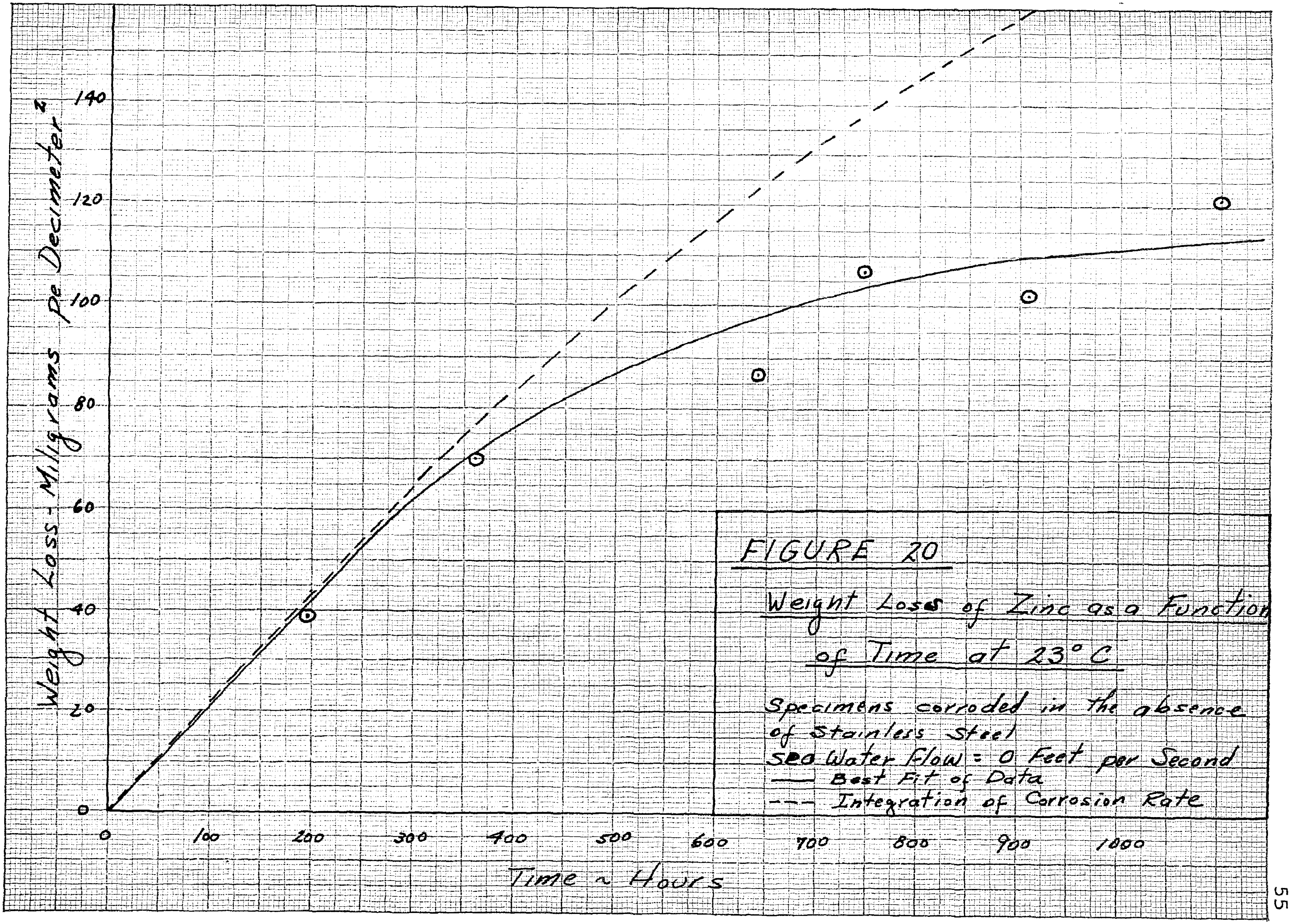

FIGURE 20

Weight Loss of Zinc as a Function of Time at 23° C

Specimens corroded in the absence of Stainless Steel
Sea Water Flow = 0 Feet per Second
—— Best Fit of Data
- - - Integration of Corrosion Rate

a slight tarnish with few pits. The corrosion rate was taken from Figure 19 at 1000 hours since the best fit curve of Figure 20 indicated an almost zero rate after 900 hours. The corrosion rate is 2.6 milligrams per square decimeter-day.

Table 7 lists the weight change data for stainless steel exposed to sea water.

TABLE 7

The Sea Water Corrosion of Stainless Steel 304 at 23°C

Time hrs	Flow Rate Ft/sec	Weight Gain mg/dm^2
	Static	
161	0	3.70
161	0	5.19
329	0	1.81
329	0	5.72
610	0	0
610	0	0
711	0	0
711	0	3.23
878	0	-1.30
878	0	-0.85
1067	0	0
1067	0	0
	Dynamic	
177	1.49	4.75
177	1.49	6.92
368	1.47	5.95
368	1.47	7.68
530	1.27	0
530	1.27	2.15
705	1.24	0
705	1.24	2.15
860	1.56	0.43
860	1.56	0
1035	1.22	4.07
1035	1.22	2.66

As can be seen from the above table, the corrosion of stainless steel 304 in sea water by itself is on the same order of magnitude as the error in the measurements and was, therefore, assumed zero. The stainless specimens did not show any indications of pitting nor of picking up the black magnetite coating described earlier for galvanically coupled samples.

DISCUSSION

The galvanic corrosion of bi-metallic couples has generally been determined by taking the difference between the corrosion rate of the members of the couple when electrically connected and subtracting the uncoupled corrosion of each. The galvanic corrosion contribution, determined in this manner is subject to many qualifications.

The corrosion rate is generally a non-linear function of time, therefore, most corrosion scientists specify a time basis for their data. This suffers from a lack of generality since it only applies for an instantaneous rate. It would be desirable to express the galvanic corrosion as an analytic function of time or to wait until the corrosion process has achieved a steady state and report the equilibrium galvanic corrosion rate. The latter method was used in this thesis.

Another assumption which is commonly accepted is that no synergistic effects over and above galvanic corrosion occurs when dissimilar metals are brought into contact. This assumption is not necessarily true. Generally, the term galvanic corrosion is redefined to mean any corrosion over the corrosion of the individual metal in the corroding medium. The latter definition was used for reporting the data in this thesis.

TABLE 8

Effect of Velocity on Galvanic Corrosion of High Purity Zinc and Stainless Steel 304 in Synthetic Sea Water.

Temperature = 23°C

Time of Test = 1000 hours

Area of Specimen = 0.222 square decimeter.

Zinc

Flow > 1.3 ft/sec

	Overall Corrosion Rate	Galvanic Contribution	Potential vrs Std. Calomel Electrode
	mdd	mdd	volts
Connected with SS 304	-237	-199	-1.058
Connected with 1/16" Sea Water Film	-187	-149	-1.072
Metal Alone	-38	-	-

Zinc

Flow = 0

	Overall Corrosion Rate	Galvanic Contribution	Potential vrs Std. Calomel Electrode
	mdd	mdd	
Connected with SS304	-18.4	-15.8	-1.068
Connected with 1/16" Sea Water Film	-17.7	-15.1	-1.074
Metal Alone	- 2.6	-	-

Stainless Steel 304

Flow >1.3 ft/sec.

	Overall Corrosion Rate	Galvanic Contribution	Potential vrs Std. Calomel Electrode
	mdd	mdd	volts
Connected with SS 304	+0.90	+0.90	-0.220
Connected with 1/16" Sea Water Film	+0.94	+0.94	-0.233
Metal Alone	0	-	-

Stainless Steel 304

Flow = 0

	Overall Corrosion Rate	Galvanic Contribution	Potential vrs Std. Calomel Electrode
	mdd	mdd	volts
Connected with SS 304	+0.53	+0.53	-0.248
Connected with 1/16" Sea Water Film	+0.50	+0.50	-0.258
Metal Alone	0	-	-

mdd = milligrams per square decimeter-day.

The corrosion of two dissimilar metals which are joined together with an electrical conductor and subjected to a flowing corrodent is a function of many factors. Some of the more important factors include temperature, electrical resistance between members of the couple, corroding medium concentration gradient, corroding medium flow rate, surface area and the potential difference of these metals in the corrodent.

The potential difference of common metals and alloys in flowing sea water was determined qualitatively by LaQue and Cox.(8) They found the potential of passivated stainless steel 304 to be cathodic to all materials while zinc was anodic to all materials except magnesium and its alloys. LaQue and Cox further report in their Table II, a literature compilation of the potentials of several metals referred to a saturated calomel electrode in salt water and similar solutions, that zinc has a potential between -1.07 and -1.09 while stainless steel 304 has a potential between -0.11 and -0.31. These numbers are in excellent agreement with those determined in this thesis (Table 8).

The corrosion area used for Table 8 was based on the initial area of the specimens. It would have been more accurate to use an experimentally determined area, since the area increased as the zinc corroded due to pitting. Ultimately, the area will decrease as more and more of a specimen is corroded away. The experimental difficulties involved in measuring surface areas are numerous, therefore, most corrosion research does not go to this refinement.

The effect of corrodent flow rate is varied and often conflicting. In general, a moving fluid tends to make corrosion conditions more uniform and prevent localized attack. But, at higher flow rates, turbulence of the fluid may produce non-uniformity which leads to pitting. In this research, the experiment was designed to determine the effect of the sea water at the inception of turbulance. The Reynolds number was estimated to be in the range of 2100 to 3500. Furthermore, fluid motion tends to accelerate corrosion by removing corrosion products from the reaction region and the other is by supplying fresh corrodent at a faster rate.

The corrosion rate of zinc in the absence of stainless steel is in good agreement with data published by Friend(7) who obtained a corrosion rate of 18 milligrams per square decimeter-day in a 4 year sea water test. He also reported that the surface was roughly pitted. Friend and Tedemus(6) reported a 64 day test for zinc in sodium chloride (5 to 300 grams per liter) resulted in a corrosion rate from 2.6 to 18. milligrams per square decimeter-day. McKay and Worthington(9) reported the following corrosion rates in salt water for zinc 3 to 50 mdd and for stainless steel 1-1000 mdd. All these values are in excellent agreement with the data of this thesis.

Care should be exercised in extrapolating salt corrosion for sea water application. Wormwell, et al(16) indicated that corrosion rates are definitely higher in a 0.5 normal sodium chloride solution than in sea water. He attributed this fact to the formation of calcium and magnesium scale due to the rise in pH at the cathodic areas.

There are other factors in addition to the one just mentioned which pertain to composition of the corroding medium. The concentration and composition of sea water can affect corrosion by influencing the rate of solution and solubility of corrosion products, influencing viscosity and density and, therefore, the rate of diffusion from the corrosion area and influencing the conductivity which would allow a longer path for the galvanic current and, therefore, faster anode corrosion. Although synthetic sea water was used in this experiment, the attempt to duplicate all the normal sea water constituents was effective, therefore, overcoming the usual objections to a synthetic blend. The effect of running the experiment at a chlorinity of 12 when most sea waters have a chlorinity of 19 is not known. It would seem that concentration is not a critical parameter in this range in view of the excellent agreement with published values.

The temperature of this study was maintained constant at 23 ± 1°C. The effect of temperature on galvanic corrosion is difficult to ascertain without experimental work. The equilibrium oxygen concentration will decrease as temperature increases, therefore, decreasing the cathode depolarization. Temperature will increase the rate of reaction, therefore, the rate of corrosion will also be expected to increase. The hydrogen overvoltage would decrease with increasing temperature. All these factors indicate an increased corrosion rate should be expected with increasing temperature.

The pH of a corroding solution is another factor which has a profound effect on corrosion. The work of Pourbaix(9) mentioned in the introduction indicates that thermodynamically there are regions where corrosion will be inhibited as a function of pH. It turns out that the pH range of sea water is the most protective for both zinc and stainless steel 304.

CONCLUSIONS

The corrosion of zinc-stainless steel 304 coupled specimens in flowing sea water does not behave in a predictable manner. One would expect zinc to act as a sacrificial anode and greatly reduce the corrosion of stainless steel. This however, is not the case. Stainless steel suffered a greater weight change when coupled to zinc. The weight change of stainless steel when corroded by itself was of the same order of magnitude as the accuracy of measuring and weighing the specimens and was, therefore, assumed zero.

The zinc specimens pitted heavily. This was observed by Friend(7) and others in corrosion of zinc by itself. In the case where the anode and cathode are physically separated, such as in metallic couples, more uniform corrosion would be expected. Pitting is generally attributed to local anodes and cathodes on the same metal. The fundamental reason for the zinc pitting when coupled to stainless steel is not known.

The accelerated corrosion rate of zinc when coupled to a noble metal such as stainless steel was expected and indeed the data of this thesis bears this out.

Although many corrosion scientists claim that stain less steel pits in sea water, this was not observed over the 1000 hour experiment.

RECOMMENDATIONS

A detailed mechanistic study of the electrochemistry of galvanic corrosion is very desirable. The study should include detailed time studies of area change and film growth. The zinc-stainless steel 304 system could be valuable for such a study since there are large overall effects providing the potential for more accurate measurements. A study of this kind should attempt to determine accurately the initial rate of corrosion. This will yield itself better to mathematical formulations of corrosion and more reliable extrapolations.

The use of radio-isotopes in the sea water and activating the zinc-stainless steel specimens with neutron irradiation presents an unusually simple and accurate method of performing the suggested research. The isotope Zn65 has a 1.12 MEV gamma ray which could be monitored continuously in a flowing solution providing a direct measure of weight loss per unit time. The isotope Cr51 can perform the same function for stainless steel with its 0.32 gamma ray. The sea water can use Na22 as a tracer which has a 1.28 gamma ray. Some preliminary calculations were made that indicate that a one hour irradiation in a reactor neutron flux of $6x10^{12}$ neutrons/cm^2-sec will give ample activity to carry on the research without causing any safety or waste disposal problems.

The surface area measurements can be made with BET apparatus. This does not answer the whole problem of surface measurement in a liquid system since most ionic species are highly hydrated and very large but will undoubtedly give more realistic values for corrosion rate.

REFERENCES

1. Bannister, C. O. "The Protective Action of Zinc Plates in Boilers", The Metal Industry (London) Vol. 41, 1932, pp. 441-443, 467-470.

2. Bengough, G. D. and R. May, "Seventh Report of the Corrosion Committee of the Institute of Metals", Journal of the Institute of Metals, Vol. 32, 1924, pp. 82-243.

3. Evans, Ulick R., "The Corrosion and Oxidation of Metals: Scientific Principles and Practical Applications. London. Edward Arnold (Publishers) Ltd. 1960.

4. Feinknecht, W. Metaux et Corrosion. Vol. 22, 1947, pp. 192.

5. Fontana, Mars. Corrosion: A Compilation. Columbus, Ohio. The Press of Hollenback. 1957.

6. Friend, J. N. and J. S. Tidmus, "The Relative Corrosion of Zinc and Lead in Solutions of Inorganic Salts", Journal of the Institute of Metals. Vol. 31, 1924, pp. 177-185.

7. Friend, J. N., "The Relative Corrodibilities of Ferrous and Non-Ferrous Metals and Alloys". Part I. The results of Four Years Exposure in the Bristol Channel", Journal of the Institute of Metals. Vol. 39, 1928, pp. 111-133.

8. LaQue, F. L. and G. L. Cox. "Some Observations of the Potentials of Metals and Alloys in Sea Water". Proceedings of the American Society for Testing Materials. Vol. 40. 1942. pp. 670.

9. McKay, Robert J., Worthington, Robert. Corrosion Resistance of Metals and Alloys. Am. Chem. Soc. Monograph Series No. 71; New York: Reinhold Publishing Corp. 1936.

10. Potter, Edmund C., Electochemistry Principles and Applications. London: Cleaver-Hume Press, Ltd. 1956.

11. Pourbaix, M. J. N (Translated by J. N. Agar) Thermodynamics of Dilute Aqueous Solutions. London: Edward Arnold (Publishers) Ltd. 1949.

12. Pray, H. A., C. E. Schweickert and B. H. Minnich. "Solubility of Hydrogen, Oxygen, Nitrogen and Helium in Water at Elevated Temperatures". Industrial and Engineering Chemistry. Vol. 44. 1952. pp. 1146-1151.

13. Speller, Frank N. Corrosion - Causes and Prevention. New York: McGraw-Hill Book Company, Inc. 1951.

14. Uhlig, H. H. The Corrosion Handbook. New York: John Wiley and Sons. 1958.

15. Whitman, W. G. and R. P. Russell. "The Natural Water Corrosion of Steel in Contact with Copper". Industrial and Engineering Chemistry. Vol. 16. 1924. pp. 276.

16. Wormwell, F., T. J. Nurse and H. C. Ison. "High Speed Rotor Tests of Paints for Underwater Service". Iron and Steel Institute (London). November 1958.